Biogeochemistry (2020) 149:115–140
https://doi.org/10.1007/s10533-020-00665-8

Benthic fluxes of dissolved oxygen and nutrients across hydrogeomorphic zones in a coastal deltaic floodplain within the Mississippi River delta plain

Song Li · Alexandra Christensen · Robert R. Twilley

Received: 2 September 2019 / Revised: 1 April 2020 / Accepted: 14 April 2020 / Published online: 7 May 2020

Abstract We tested the hypothesis that benthic fluxes will increase spatially in a coastal deltaic floodplain as sediment organic matter increases in response to developing hydrogeomorphic zones along a chronosequence of the active Mississippi River Delta. A continuous flow-through core system was used to incubate intact sediment cores from three hydrogeomorphic zones along a chronosequence in the emerging Wax Lake Delta (WLD). Organic matter content increased from younger to older deltaic sediments from subtidal to supratidal hydrogeomorphic zones, which were coupled with increasing benthic oxygen and nitrogen fluxes. Mean net denitrification rate in spring was 100 μmol N_2–N m^{-2} h^{-1} with significantly lower rates occurring in the younger intertidal zones (T4 transect, − 22 μmol N_2–N m^{-2} h^{-1}) and higher rates occurring in the older supratidal zones (T2 and T1 transects, 330 and 262 μmol N_2–N m^{-2} h^{-1}, respectively). Mean net denitrification rate in summer was 397 μmol N_2–N m^{-2} h^{-1} without significant site-to-site variability except for the supratidal-T2 site (911 μmol N_2–N m^{-2} h^{-1}) showing higher denitrification rate than the other sites. Based on seasonal temperature and inundation time, annual rates of benthic NO_3^- removal varied from − 0.5 to − 3.4 mol m^{-2} y^{-1} and N_2–N production rates varied from 1.0 to 3.2 mol N m^{-2} y^{-1} across WLD. The subtidal zone had the lowest fluxes associated with lower organic matter content, but was the hydrogeomorphic zone with the largest area and longest flood duration, and therefore contributed over half of N removal in WLD. The estimated annual NO_3^- removal of 896 Mg N y^{-1} in WLD accounts for 10 to 27% of total NO_3^- load to WLD, most of which is converted to N_2 through denitrification. As a small prograding coastal deltaic floodplain under early stages of delta development, WLD is a continuously emerging ecosystem where the capacity of N removal increases by 0.2 to 2% per year prior to riverine NO_3^- is export to coastal ocean. These results highlight the contribution of the coastal deltaic floodplain in an active coastal basin in processing elevated riverine NO_3^- at continental margins with coastal ocean. The potential loss of this ecosystem service in N removal may increase in global significance as delta areas decline as result of accelerated relative sea level rise and decreased sediment loading in major river basins around the world.

Keywords Coastal deltaic floodplain · Benthic fluxes · Denitrification · Sediment oxygen

Responsible Editor: J. M. Melack

S. Li (✉) · A. Christensen · R. R. Twilley
Department of Oceanography and Coastal Sciences, College of the Coast and Environment, Louisiana State University, Baton Rouge, LA 70803, USA
e-mail: sli10@lsu.edu

R. R. Twilley
Louisiana Sea Grant, Louisiana State University, Baton Rouge, LA 70803, USA

consumption · Hydrogeomorphic zones · Nitrogen removal

Introduction

The application of nitrogen (N) fertilizers to agricultural fields has increased by about 800% over the last several decades, but agricultural N use efficiency has remained below 40% (Fixen and West 2002; Canfield et al. 2010). As a result, significant amounts of inorganic N leach into rivers, causing a two to four-fold increase in nitrate (NO_3^-) concentrations since 1960 in estuarine and coastal ecosystems in North America (Goolsby et al. 2000; Rabalais et al. 2002; Howarth et al. 2002). Meanwhile, coastal phosphorus (P) concentrations have increased due to anthropogenic fertilization and industrial wastewater (Conley et al. 2009). The elevated loads of inorganic N and P enhance coastal net primary productivity, stimulate harmful algal blooms, decrease water quality, and exacerbate hypoxia (oxygen depletion < 2 mg l^{-1} in bottom water) (Rabalais et al. 2002; Paerl et al. 2002; Diaz and Rosenberg 2008).

Elevated inorganic nutrient concentrations in river basins have stimulated research on how patterns of denitrification in alluvial floodplains may reduce the potential for eutrophication of downstream ecosystems (Goolsby et al. 2000; Noe and Hupp 2009; Jordan et al. 2011). Less information is available on the significance of coastal deltaic floodplains in reducing eutrophication at continental margins with major rivers. Coastal deltaic floodplains form in the deposition zone where major rivers reach the ocean, representing wetlands at the interface of land and oceans (Henry and Twilley 2014; Hiatt and Passalacqua 2015; Bevington and Twilley 2018). Similar to alluvial floodplains, coastal deltaic floodplains are also depositional environments connected to rivers, but multiple factors like tides, waves, tropical storms and meteorological fronts make the geomorphology and connectivity (daily and seasonal inundation) between channels and coastal deltaic floodplains more complex in comparison to alluvial floodplains (Twilley et al. 2019). The morphological development of coastal deltaic floodplains results in spatial and temporal differences in elevation, vegetation, and sediment organic matter content (Lorenzo-Trueba et al. 2012; Carle 2013; Bevington and Twilley 2018). Soil elevations of different hydrogeomorphic zones favor specific vegetation communities and generate different rates of organic matter accumulation (Bevington and Twilley 2018).

Recent research reported that patterns of hydrogeomorphology along longitudinal zones of major river systems control the processing of NO_3^- in alluvial floodplains (Clawson et al. 2001; Noe and Hupp 2005; Welti et al. 2012; Noe et al. 2013). However, the influence of hydrogeomorphic zones in processing nutrients in a coastal deltaic floodplain has not been resolved compared with alluvial floodplain ecosystems. As hydrogeomorphic zones age during active deltaic development, benthic ecological and biogeochemical processes may change, representing a chronosequence of ecosystems (Twilley et al. 2019). Previous work in our research group indicated that benthic nutrient fluxes did vary along the deltaic chronosequence, but these findings did not clearly differentiate the influence of hydrogeomorphic zones (Henry and Twilley 2014). More information on landscape patterns of benthic fluxes is required to further understand the role of active coastal deltaic floodplains in permanent NO_3^- removal in response to both the chronosequence and hydrogeomorphic variations.

Denitrification is an ecologically important pathway to permanently remove bio-reactive N under anaerobic condition(Cornwell et al. 1999; Piña-Ochoa and Álvarez-Cobelas 2006; Eyre and Ferguson 2009; Scaroni et al. 2011; Henry and Twilley 2014). Denitrification is categorized as 'direct denitrification' that reduces external NO_3^- to N_2 gas and 'coupled nitrification-denitrification' that uses NO_3^- generated by in situ nitrification. Determination of denitrification is impeded by methodological difficulties from high background N_2 concentrations and large spatial and temporal heterogeneity of N_2 production in coastal ecosystems (Cornwell et al. 1999; Davidson and Seitzinger 2006). Previous research on benthic nutrient fluxes estimated denitrification indirectly based on a stoichiometric assumption that the molar organic carbon (C):oxygen (O) and N:P ratios of sediment fluxes should follow Redfield composition (C:O:N:P = 106:138:16:1). A discrepancy between measured O:N:P ratio of these elements exchanged at the sediment-water interface compared to the expected

Redfield ratio may reflect the occurrence of benthic denitrification (Nielsen 1992; Kana et al. 1994; Gilbert et al. 1997; Cornwell et al. 1999). Recent improvements in direct techniques such as N_2:Ar method and isotope pairing technique have demonstrated the significance of benthic fluxes to N_2 production (Seitzinger et al. 1984; Gardner and McCarthy 2009; Henry and Twilley 2014). The direct measurements of benthic denitrification are reported to be correlated with indirect estimates of denitrification using stoichiometric assumption in Massachusetts Bay (Giblin et al. 1995, 1997). However, the correlation of estimated benthic denitrification rates with directly measured rates is not well clarified in most coastal regions. To get a general idea of the relationship between benthic dissolved inorganic N (DIN = $NH_4^+ + NO_3^- + NO_2^-$) fluxes and denitrification rates, it is important to investigate if the estimated denitrification rates from stoichiometric assumptions give comparable rates as directly measured denitrification rates in coastal ecosystems.

Here, we compared the spatial and seasonal patterns of nutrient processing in coastal deltaic floodplains as a function of hydrogeomorphology and delta age since emergence. We hypothesized that benthic fluxes of dissolved oxygen (O_2), N_2 and inorganic nutrients will increase in a newly emergent coastal deltaic floodplain from lower to higher hydrogeomorphic zones and from younger to older chronosequence within each hydrogeomorphic zone. We used seasonal measures of benthic fluxes and denitrification rates across hydrogeomorphic zones with different hydroperiods (duration of inundation per year) to estimate the annual NO_3^- removal and N_2 release in a coastal deltaic floodplain at the mouth of the Atchafalaya River. We compared the estimates of denitrification using stoichiometry of benthic fluxes with direct measures of N_2 production to test assumptions of denitrification rates using different methodologies in deltaic environments. This analysis will describe the role of newly emergent deltaic floodplains in NO_3^- removal from riverine loading compared to other ecosystems of the Mississippi River Delta Plain.

Methods

Experimental design

Wax Lake Delta (WLD) is an emergent coastal deltaic floodplain in the Atchafalaya Coastal Basin within the Mississippi River Delta (Fig. 1). The U.S. Army Corps of Engineers constructed the Wax Lake Outlet (WLO) in 1941 to divert flow from the Atchafalaya River and provide flood relief to Morgan City, Louisiana. Riverine sediments carried by WLO began to form a subaqueous delta at the outlet mouth upon completed construction. In 1973, an unusually high spring flood resulted in large sediment deposition and WLD became subaerial (Roberts et al. 2003). Deltaic islands emerged rapidly throughout the next several decades at a rate of about 1 to 5 km^2 y^{-1} with a minor anthropogenic influence from navigation (Roberts et al. 1997; Wellner et al. 2005; Allen et al. 2012; Carle et al. 2015). WLD provides a natural laboratory to study the ecological succession and biogeochemistry of a coastal deltaic floodplain and to test the hypotheses presented concerning chronosequence, elevation and sediment organic matter content (Henry and Twilley 2014; Bevington and Twilley 2018).

Experimental sites were selected on Mike Island (Fig. 1), a well-developed island of WLD, to test the hypotheses of benthic fluxes with hydrogeomorphology. Three hydrogeomorphic zones were defined on the basis of sediment surface elevations from USGS Atchafalaya 2 Project LiDAR Survey 2012 (4 m resolution, Bevington and Twilley 2018). Area with sediment surface elevation lower than mean low water (MLW, − 0.04 m NAVD 88) is a subtidal zone while area with elevation higher than mean high water (MHW, 0.30 m NAVD88) is a supratidal zone. Area with sediment surface elevation between MLW and MHW is an intertidal zone. The area of each hydrogeomorphic zone was calculated based on a digital elevation model (DEM) of Mike Island (Bevington and Twilley 2018). The subtidal zone is the dominant hydrogeomorphic zone on Mike Island followed by the intertidal zone and the supratidal zone. Subaqueous areas below − 0.75 m NAVD 88 were excluded. The subtidal zone has a molar organic carbon to total nitrogen (C:N) ratio of 9:7 in the top 4 cm of soil, whereas the supratidal and intertidal zones show larger C:N ratios of 11:6.

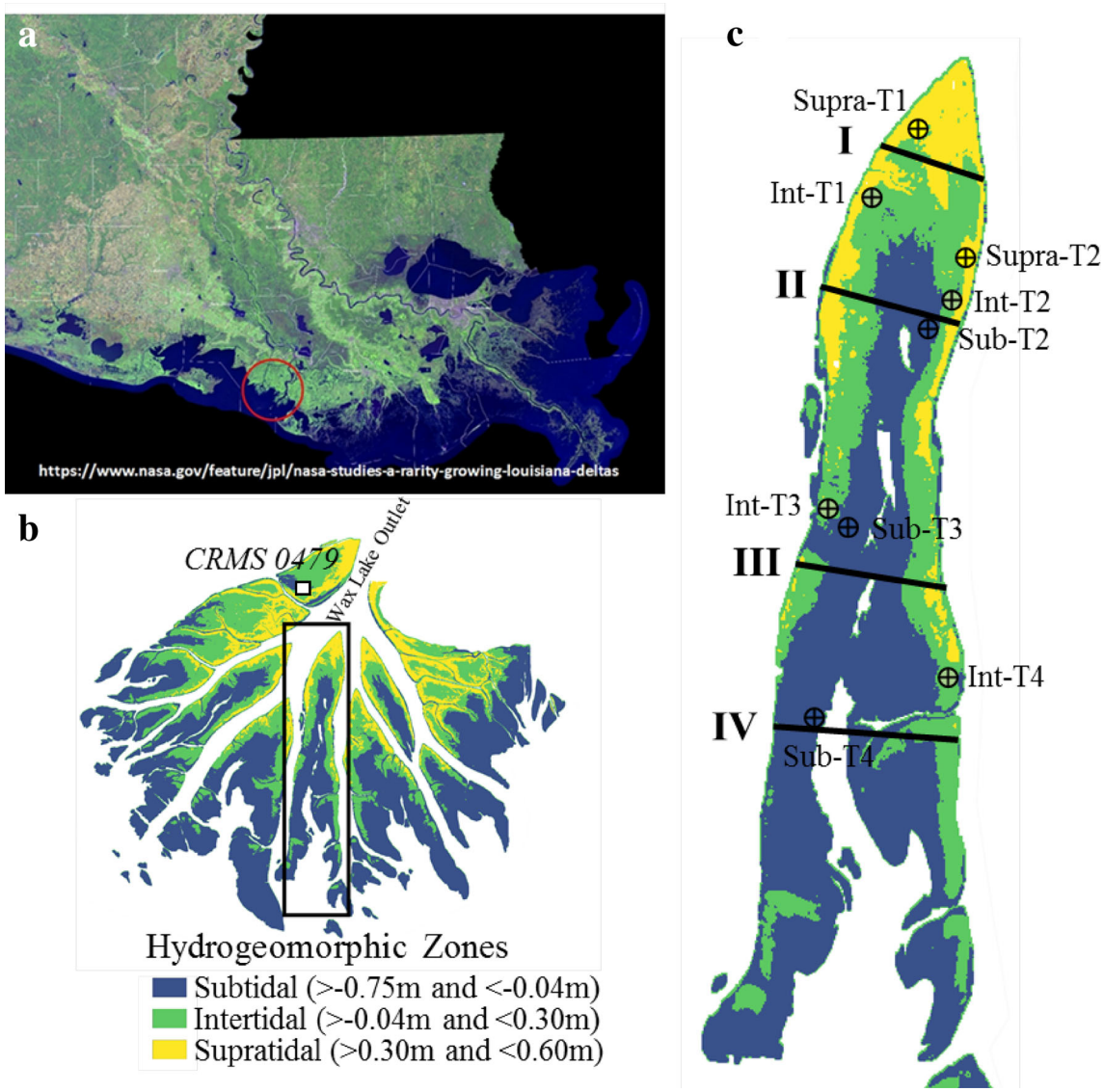

Fig. 1 Map of Mike Island in Wax Lake Delta (WLD), Louisiana, with the location of study sites. Elevation records are from USGS Atchafalaya 2 project LiDAR Survey 2012 digital elevation model (4 m resolution). The black lines across Mike island delineate four chronosequence transects (from younger to older: T4 to T1) mainly defined by the distance to apex of Mike Island and the characterization of cross-sectional morphology (Bevington and Twilley 2018). Three hydrogeomorphic zones (subtidal, intertidal, and supratidal) are distinguished by sediment surface elevation relative to mean high water (MHW) and mean low water (MLW). White square in WLD indicates the location of CRMS 0479 station established by the Coastal Resources Monitoring System (CRMS) to measure water temperature

The chronosequence zones along Mike Island were defined based on a conceptual model from Bevington and Twilley 2018) Briefly, island morphology and elevation development are controlled primarily by island age. Four chronosequence zones were thus determined depending on the distance to delta apex and the characterization of cross-sectional morphology (Bevington and Twilley 2018). Transect I (T1) is $\geq$ 35 years since emergence and is dominated by the supratidal zone with higher elevations ($\geq$ 0.3 m), while transect II (T2) is estimated at 20–35 years since emergence and dominated by the intertidal zone. Transects III and IV (T3 and T4) are younger zones ($\leq$ 20 year since emergence) of Mike island

Table 1 Site distributions and sampling dates in different hydrogeomorphic and chronosequence zones in Wax Lake Delta (WLD), Louisiana

Hydrogeomorphic	Chronosequence			
	T4	T3	T2	T1
	Younger	→		Older
Subtidal	Mar. 2018 Aug. 2017	Mar. 2018 Aug. 2017	Mar.2018 Jul.2017	NA*
Intertidal	Mar. 2018 Jul. 2017	Mar. 2018 Aug. 2017	Mar.2018 Jul.2017	Feb.2018 May 2017
Supratidal	NA*	NA*	Feb. 2018 May 2017	Feb.2018 Jul.2018

*No data available for these hydrogeomorphic and chronosequence combinations

dominated by the subtidal zone with a lower slope from levee ridge to the interdistributary bay.

Nine experimental sites were selected in three hydrogeomorphic zones (subtidal, intertidal and supratidal) along four chronosequence zones (Fig. 1; Table 1). There was an uneven distribution of experimental treatments of hydrogeomorphic zones within the four chronosequence zones. For example, the intertidal zone was the only hydrogeomorphic zone that occurred in all chronosequence zones (T1–T4). The subtidal zone did not occur in the older region of Mike Island (T1) while the supratidal zone was mostly absent in the younger zones of Mike Island (T3 and T4). The assignment of experimental sites to a hydrogeomorphic zone were confirmed with elevations (NAVD 88) based on real-time kinematic (RTK) positioning using a Trimble R8 GNSS. Supratidal-T2 did not have available elevation measurements nearby, so its elevation was roughly estimated from a digital elevation model (m NAVD 88; LiDAR Survey 2012; Bevington and Twilley 2018).

Ambient Conditions

Replicate porewater (4 cm depth) and surface water (within top 5 cm of the air-water interface) samples were collected at each experimental field site to capture sediment and overlying water characteristics of hydrogeomorphic and chronosequence zones. Water samples were stored on ice and filtered through GF/F glass microfiber filters (25 mm diameter, 0.7 µm particle retention) immediately upon arrival at the laboratory. Samples were stored in a freezer (− 20 °C) until dissolved inorganic nutrients [ammonium (NH_4^+), nitrite (NO_2^-), nitrate (NO_3^-) and phosphate (PO_4^{3-})] were determined on a flow solution IV autoanalyzer (OI analytical, College Station, Texas). Temperature and salinity of surface water and porewater were measured immediately after collection in the field with a YSI salinity-conductivity-temperature meter. Benthic incubations.

Triplicate sediment cores (10 cm internal diameter by 20 cm depth) were collected randomly in each of the nine experimental sites to measure nutrient fluxes at the sediment-water interface. Cores were collected during two different seasons representing cooler temperatures in spring (February and March 2018) and warmer temperatures in summer (May to August 2017). In summer 2017, supratidal-T1 was skipped for technical reasons, but it was collected in summer 2018. Aboveground vegetation was excluded when collecting intact sediment cores, but rhizomes, roots, infauna and benthic algae were included. Headspace over the sediment in each core was carefully adjusted to 10 ± 1 cm in height. The cores were sealed using silicone-greased bottoms, then gently filled with ambient water in the field. Cores were stored in a cooler under in situ temperature and transported back to the laboratory. Ambient water was collected from WLO at the Calumet boat launch, LA, representing river water flowing to WLD. For incubation conditions, ambient water was filtered using a five-stage filtration system (30, 20, 5, 1, and 0.2 µm) and used to gently replace overlying water inside sediment cores with minimal disturbance to the sediment-water interfaces in the laboratory. Using filtered water

during incubations excludes most microbial processes in the overlying water column and attributes changes in nutrient concentrations, dissolved O_2 and N_2 gases to benthic processes (Miller-Way and Twilley 1996). The top of each core was sealed with a lid containing inlet and outlet tubing and affixed with a magnetic stir bar to gently mix the overlying water. The sealed cores were incubated in a water chamber at controlled temperatures of either 12 °C for spring months or 22 °C for summer months.

All the incubations were conducted in the dark with a continuous flow-through system (Miller-Way and Twilley 1996). Sediment cores were connected to water reservoirs through inlet tubing with a peristaltic pump controlling the flow rate at 2.4 ± 0.2 ml min^{-1} in spring (residence time = 6 h) and 4.6 ± 0.5 ml min^{-1} in summer (residence time = 3 h). The flow rate in each season was determined through previous experiments performed at the corresponding temperature in each season. We chose an overlying water residence time that was long enough to produce a measurable difference between influent and effluent concentrations, but short enough to support an aerobic condition with dissolved O_2 concentration $\geq$ 3 mg l^{-1} in each season (Miller-Way and Twilley 1996). At the optimal and constant flow rate in each season, the continuous flow-through system achieved steady state conditions inside sediment cores (non-varying flux with time), which indicated representative benthic fluxes in each site (Miller-Way and Twilley 1996). Cores were pre-incubated for at least three turnover times of the overlying water in the cores (about 18 h in spring and 9 h in summer) to allow fluxes at the sediment-water interface to reach an equilibrium.

After the pre-incubation period, influent and effluent water was collected to measure inorganic nutrients, dissolved O_2 and N_2 gas concentrations at the completion of a single water residence time for a total of three turnovers per experiment. Two blank cores with only filtered ambient water were incubated for each experiment in each season to correct all possible interferences not related to changes in nutrient concentrations due specifically to benthic activities. Water samples were filtered immediately through 25 mm GF/F glass microfiber filters into triplicate vials (20 ml) and stored in a freezer (− 20 °C) until analyzed for NH_4^+, NO_2^-, NO_3^- and PO_4^{3-} on the OI autoanalyzer. Replicate samples for dissolved gas analysis were collected in 12 ml gas-tight exetainers (Labco Limited, Lampeter, Wales, UK). After each exetainer was filled, 200 µl of $ZnCl_2$ solution (50% of saturation concentration) was injected (Nielsen and Glud 1996), and the exetainer was tightly capped immediately. The gas samples were then stored under water in a water bath at 4 °C. Dissolved N_2 was measured in a membrane inlet mass spectrometer (MIMS) within one month (precision < 0.03%; Kana and others 1994). Benthic fluxes of inorganic nutrients and dissolved gas (N_2 and O_2) were determined by the equation:

$$\text{Flux} = \frac{[(\text{Co} - \text{Ci}) - (\text{Cbo} - \text{Cbi})] \cdot \text{flow rate}}{\text{Core surface area}} \quad (1)$$

where Co and Ci (µM) refer to outflow and inflow concentrations of a sediment core while Cbo and Cbi (µM) are the average outflow and inflow concentrations of two blank cores in corresponding incubation events.

The top 4 cm of sediment in each core was sampled with a piston core (2.4 cm internal diameter) and segmented at 2 cm depth intervals. Each slice of sediment was oven-dried at 60 °C to a constant mass and bulk density was measured by dividing dry sediment mass by sediment volume (8.75 cm^3). Each dried sediment sample was ground to less than 250 µm in a Wiley Mill, and a 1 ± 0.01 g subsample was ignited at 550 °C for 2 h to estimate organic matter content.

Scaling benthic fluxes to annual rates

Incubations for cores sampled in early spring were controlled at 12 °C, compared to 22 °C for cores sampled in summer. The median of these two temperatures (17 °C) was used to define ambient water temperatures into either summer or spring seasons. The study area is in the warm temperate region with annual surface water temperatures ranging from 5.6 to 31.3 °C. Here we assumed the study area has only two seasons per year, spring and summer, when water temperatures are less than or no less than 17 °C, respectively. Annual spring days and summer days were calculated from daily water temperature measurements at Coastal Recourses Monitoring System (CRMS) station 0479 (29° 31.4′ N, 91° 27.0′ W)

located in the intertidal zone of WLD, from May 2017 to April 2018 (recognized as an experimental year). There are several days showing undefined water temperature during this period. We used water temperature readings in the same dates, but one or two years ahead, to fill in these missing values. We assumed the supratidal and subtidal zones had the same water temperature as the intertidal zone when submerged. The hydroperiod for each experimental site (hours inundated per day) from May 2017 to April 2018 was based on continuous water level records from a tidal gauge near WLD (29° 27.0′ N, 91° 20.3′ W, Amerada Pass, LA). The difference between the sediment surface elevation of the tide gauge and the sediment surface elevation of an experimental site was compared to continuous water level records to determine daily inundation time in each experimental site. Summer NO_3^- and N_2–N fluxes were applied only if the site was inundated and, meanwhile, the overlying water was at or above 17 °C. Spring NO_3^- and N_2–N fluxes were applied if the site was inundated and the overlying water was below 17 °C.

Statistical analyses

Repeated measures analysis of variances (ANOVAs) were used to test the difference in nutrients, dissolved O_2 and N_2 fluxes among experimental sites in each of the sampling season. We used repeated measures for the three repeated sampling events of an individual core over time to confirm that each core achieved a steady state (no significant difference over time in each core) during the sampling period (Miller-Way and Twilley 1996). Seasonal differences were tested using one-way ANOVA by treating the results from the nine experimental sites in each season as a whole and ignoring site-to-site variations. Significant differences were also tested on the interaction between seasons and hydrogeomorphic zones with chronosequence results nested in each hydrogeomorphic zone using ANOVA. When differences were significant at a 95% confidence level, Tukey's HSD post hoc test was used to do all pairwise comparisons and letters designated significant differences ($p < 0.05$). Data analyses were performed using SAS and JMP software. Benthic fluxes were presented as means with error bars of standard error (SE).

Results

Sediment Properties and Benthic Fluxes

WLD was a tidal freshwater system with surface water salinity ranging from 0.1 to 0.2 and porewater salinity ranging from 0.2 to 0.4 (Table 2). Ambient NO_3^- concentrations of *in-situ* surface water varied from 0.1 to 50.8 μM in spring and from 0.1 to 84.1 μM in summer. Site-to-site variations in overlying NO_3^- concentrations demonstrated different NO_3^- removal capacities from different experimental sites to process riverine nutrients from the same water source (WLO). Ambient NH_4^+ concentrations varied from 0.7 to 6.5 μM in surface water, which were lower than porewater NH_4^+ concentrations from 5.0 to 470.9 μM in respective experimental site in each season. Ambient NO_2^- and PO_4^{3-} concentrations in surface water and porewater were generally low in all the experimental sites in the field.

Bulk density and organic matter content in the top 4 cm of sediment exhibited significant differences ($F = 130.6$, $P < 0.001$ and $F = 120.9$, $P < 0.001$, respectively) along the chronosequence of each hydrogeomorphic zone (Fig. 2), but no significant difference between seasons (Table 3). Chronosequence-averaged bulk density decreased while organic matter content increased as elevation increased from subtidal to supratidal zones in each season (Table 3). Bulk density decreased from 1.5 to 0.3 g cm^{-3} while organic matter content increased from 2.2 to 10.7% from younger (T4) to older (T2) chronosequence sites in the subtidal zone (Fig. 2). Similar patterns were observed in the intertidal zone with bulk density decreasing from 1.56 to 0.40 g cm^{-3} and organic matter increasing from 2.4 to 10.0% from the younger (T4) to the older (T1) sites. Trends in bulk density and organic matter in the two supratidal sites were different from those in the subtidal and intertidal zones. The supratidal-T1 (site near island apex) was assumed to be the older site but exhibited higher bulk density (0.9 g cm^{-3}) and lower organic matter content (8.5%) than the younger supratidal-T2 site (0.3 g cm^{-3} and 18.2%, respectively).

Benthic dissolved O_2 fluxes ranged from − 0.2 to − 3.5 g O_2 m^{-2} d^{-1} and fluxes in spring were lower than fluxes in summer (Fig. 3a). In spring, dissolved O_2 consumption increased from the younger (T4) to older (T2) chronosequences in the subtidal zone. The

chronosequence-averaged fluxes of dissolved O_2 in the subtidal and intertidal zones were significantly lower than the chronosequence-averaged flux in the supratidal zone in spring (Table 3, $P < 0.001$). In summer, there was no obvious hydrogeomorphic or chronosequence variation except for the supratidal-T2 site with significantly higher dissolved O_2 consumption of − 3.5 g O_2 m^{-2} d^{-1} ($F = 15.7$, $P < 0.001$).

Benthic fluxes of N_2 gas ranged from − 22 to 911 μmol N_2–N m^{-2} h^{-1} with a dominance of positive rates resulting from net denitrification (Fig. 3b). N_2 gas fluxes in spring were significantly lower than fluxes in summer ($F = 82.1$, $P < 0.001$). In spring, N_2 fluxes increased along the chronosequence as deltaic sediments increased in organic matter content in the subtidal and intertidal zones. Chronosequence-averaged N_2 fluxes from the subtidal and intertidal zones were significantly lower than chronosequence-averaged flux from the supratidal zones in spring (Table 3, $P < 0.001$). In summer, no obvious chronological or hydrogeomorphic variations were observed, but N_2 fluxes in the supratidal-T2 site were much higher than fluxes in the other sites.

NO_3^- concentrations in overlying water during the incubations ranged from 39.5 to 71.9 μM in spring and from 67.5 to 105.5 μM in summer (Table 4). Benthic NO_3^- fluxes were mostly negative (sediment uptake) in both seasons with a range of − 1439 to 40 μmol m^{-2} h^{-1} (Fig. 4a). In spring, benthic NO_3^- fluxes increased from the younger to older chronosequences in the subtidal and intertidal zones. Chronosequence-averaged NO_3^- flux in the subtidal zone was lower than chronosequence-averaged fluxes in the intertidal and supratidal zones in spring (Table 3). In summer, NO_3^- fluxes were significantly higher than fluxes in spring ($F = 38.0$, $P < 0.001$) and there was no significant chronosequence variation in each hydrogeomorphic zone. However, the supratidal-T2 site indicated much higher benthic NO_3^- removal than the other sites. NO_2^- fluxes varied from − 3 to 11 μmol m^{-2} h^{-1} in spring and from 2 to 67 μmol m^{-2} h^{-1} in summer (Fig. 4b). There was no significant chronosequence variation in each hydrogeomorphic zone, but the supratidal-T2 site in summer showed significantly higher NO_2^- release than other sites ($F = 10.7$, $P < 0.001$).

NH_4^+ concentrations in the overlying water during incubations varied from 1.2 to 4.0 μM in spring and 0.3 to 1.0 μM in summer (Table 4). Benthic NH_4^+ fluxes were mostly positive in both seasons (− 34 to 216 μmol m^{-2} h^{-1}), representing a net release of NH_4^+ from sediments to the water column (Fig. 5a). In spring, NH_4^+ fluxes significantly increased from the younger (T4) to the older (T2) chronosequences in the subtidal zone ($P < 0.05$). A similarly increasing pattern was observed in the intertidal zone along the chronosequence except for the intertidal-T1 site in spring. NH_4^+ fluxes in the subtidal and intertidal zones were positive, whereas fluxes in the supratidal zone were negative in spring. In summer, NH_4^+ fluxes increased along the chronosequence from the younger sites (T4) to the older sites (T2 or T1) in the subtidal and intertidal zones. Chronosequence-averaged NH_4^+ flux in the supratidal zone was lower than fluxes in the other two hydrogeomorphic zones in both seasons (Table 3). PO_4^{3-} fluxes were variable with no notable trend in either season (Fig. 5b).

Significant positive relationships were observed between sediment organic matter content and dissolved O_2, N_2–N and NO_3^- fluxes, respectively, in both seasons ($P < 0.0001$; Fig. 6). Note that the slope in the fitted equation between organic matter content and N_2–N flux in summer was about twice the slope in the fitted equation in spring (Fig. 6b). Such seasonal patterns were even obvious in the correlation of organic matter content and NO_3^- flux, as the slope in summer (− 66.8) was about 5-times larger than the slope in spring (− 12.9, Fig. 6c). In summary, benthic fluxes of N_2–N and NO_3^- were more sensitive to increases in sediment organic matter content in summer than in spring.

Scaling N fluxes to annual rates

We used 17 °C as a critical value of water temperature to categorize each day in a year in WLD as either spring or summer seasons. Overall, there were 225 days defined as summer and 140 days defined as spring during the experimental year (May 2017 to April 2018). Sites from different hydrogeomorphic zones had distinct seasonal patterns of inundation depending on topography (Fig. 7). Generally, subtidal sites were submerged for over 97% of the year, while intertidal sites were inundated more than 80% of the year, compared to < 50% for supratidal sites.

Annual rates of NO_3^- removal and N_2–N production were estimated by converting hourly NO_3^- and N_2–N fluxes into daily rates based on how long the

Table 2 Ambient surface water and porewater conditions in experimental sites in Wax Lake Delta (WLD), Louisiana

Variable		Spring								
		Subtidal			Intertidal				Supratidal	
		T4[b]	T3[b]	T2[b]	T4[c]	T3[c]	T2[c]	T1[a]	T2[a]	T1[a]
Temp (°C)	Porewater	19.1	19.3	22.8	16.2	16.6	18.3	27.9	27.3	26
	Surface water	15	16.3	24.2	15.4	15.2	15.6	29.6	NA	NA
Salinity	Porewater	0.3	0.2	0.2	0.3	0.4	0.2	0.2	0.4	0.4
	Surface water	0.1	0.1	0.1	0.1	0.1	0.1	0.1	NA	NA
NO_3^-(μM)	Porewater	25.7	6.3	0.6	17.9	0.1	0	0.1	0	1.1
	Surface water	37.9	38	10.2	50.8	49.8	43.5	0.1	NA	NA
NO_2^-(μM)	Porewater	1.3	0.3	0	1.7	0.1	0.4	0.1	0.1	0
	Surface water	1.4	1.4	0.8	0.7	0.7	0.7	0.1	NA	NA
NH_4^+(μM)	Porewater	131.5	122.1	150.6	52	171.9	50.3	147.7	101.7	27.9
	Surface water	4.9	5.3	3.8	4.5	3.4	3.3	1.7	NA	NA
PO_4^{3-}(μM)	Porewater	0.5	0.4	0.7	2	1.1	1.3	0.6	0.7	0.9
	Surface water	1.3	1.3	2.8	1	1	1.1	12.7	NA	NA
Variable		Summer								
		Subtidal			Intertidal				Supratidal	
		T4[f]	T3[f]	T2[e]	T4[e]	T3[f]	T2[e]	T1[d]	T2[d]	T1[g]
Temp (°C)	Porewater	27	28.5	30.8	38.1	28.2	38.3	23.6	24	33.7
	Surface water	27.2	27.5	29.5	35.4	26.2	30.6	25.2	NA	NA
Salinity	Porewater	0.2	0.4	0.4	0.2	0.3	0.2	0.2	0.2	0.4
	Surface water	0.2	0.2	0.2	0.2	0.2	0.2	0.2	NA	NA
NO_3^- (μM)	Porewater	38.7	4.5	0.2	77.1	38	0.9	2.1	1.5	0.3
	Surface water	64.5	63	0.1	71.7	66.7	0.3	84.1	NA	NA
NO_2^-(μM)	Porewater	0.7	0.5	0	0.1	1.2	0.1	0	0	0
	Surface water	0.3	0.4	0.1	0.2	0.3	0	1.1	NA	NA
NH_4^+(μM)	Porewater	23.9	112.7	92.5	5.0	126.4	90.3	470.9	12.6	19.1
	Surface water	1.6	0.7	1.6	1.2	1.9	1	6.5	NA	NA
PO_4^{3-}(μM)	Porewater	1.3	0.8	1.6	1.2	0.7	0.8	0.4	0.3	0.9
	Surface water	2.6	2	6.3	2.6	2.4	5.6	0.8	NA	NA

*Supra-T1 and Supra-T2 had no surface water records because the water level was zero;

*Superscripts over the chronosequence refer to sampling dates: [a]Feb 16, 2018; [b]Mar 2, 2018; [c]Mar 21, 2018; [d]May 23, 2017; [e]July 26, 2017; [f]Aug 14, 2017; [g]Jul 20, 2018

experimental sites were inundated and whether the inundation time was recognized as spring or summer. The sum of daily rates in the experimental year provided a rough estimate of annual N fluxes. The intertidal-T1, rather than the supratidal-T2, was the most significant site in removing NO_3^- (− 3.4 mol m^{-2} y^{-1}) and releasing N_2–N (3.2 mol m^{-2} y^{-1}) on the annual basis when considering seasonal temperature and annual inundation (Fig. 8). The lowest annual NO_3^- removal (− 0.5 mol m^{-2} y^{-1}) occurred at the younger intertidal zone, and the lowest N_2–N production (1.0 mol m^{-2} y^{-1}) was at the younger intertidal and subtidal zones of WLD. Over 90% of annual NO_3^- loss and N_2–N production occurred during the summer season when water temperatures were at or above 17 °C while less than 10% of these fluxes occurred during the spring season.

To calculate total N removal in WLD, the annual NO_3^- and N_2–N fluxes from different chronosequences within a certain hydrogeomorphic zone were averaged and multiplied by the total area of each hydrogeomorphic zone in WLD. The three hydrogeomorphic zones are distributed in the 50.0 km^2 WLD as 66.3% subtidal zone, 23.9% intertidal zone and

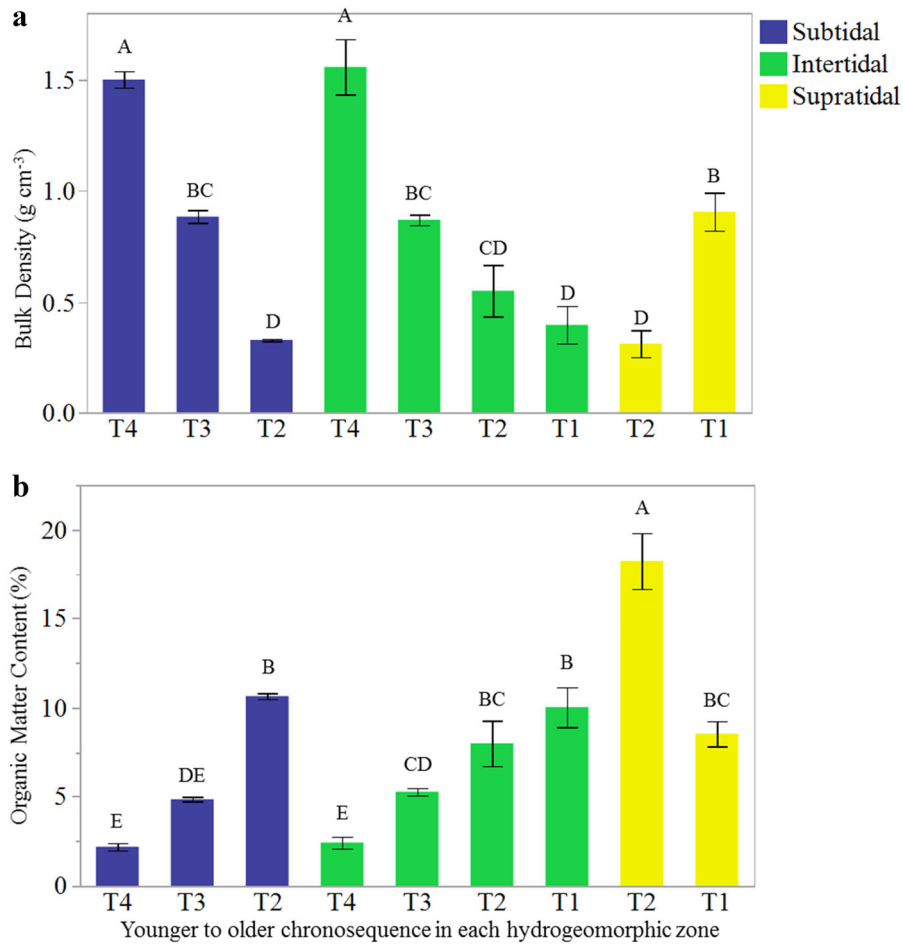

Fig. 2 Bulk density (**a**) and sediment organic matter content (**b**) in the top 4 cm of sediment among hydrogeomorphic zones (subtidal, intertidal, and supratidal) along a chronoseqeunce of younger (T4) to older (T1) sites within each hydrogeomorphic zone (mean ± 1 SE, n = 03). One-way ANOVA was used to test the difference among experimental sites and letters designate significant ($p < 0.05$) differences using Tukey's HSD test

9.8% supratidal zone (Fig. 9a). We estimated the subtidal, intertidal and supratidal zones could remove 520, 254 and 122 Mg N y^{-1} of NO_3^-, respectively, for a total of 896 Mg N y^{-1} (Fig. 9b). WLD released N_2–N to the atmosphere at rates of 712 Mg N y^{-1} from the subtidal zone, 324 Mg N y^{-1} from the intertidal zone, and 116 Mg N y^{-1} from the supratidal zone (Fig. 9c). This budget of N fluxes for this coastal deltaic floodplain suggests that there was an additional source of N, other than NO_3^- uptake, that contributed to N_2 production to the atmosphere.

Discussion

The role of organic matter content in benthic N fluxes

Combining results across hydrogeomorphic and chronosequence zones demonstrated a pattern of increased sediment organic matter content with decreased bulk density (Fig. 10). Wetland soil formation in a coastal deltaic floodplain is a process of mineral sedimentation promoting increased elevation with time that transforms subtidal to intertidal hydrogeomorphic zones (Bevington and Twilley 2018; Twilley et al. 2019). The increase in elevation as wetland soils age during delta formation causes a shift in wetland vegetation that increases the organic matter production (both aboveground and belowground),

Table 3 Characteristics of the three hydrogeomorphic zones (subtidal, intertidal and supratidal) in spring and summer based on chronosequence-averaged results in each hydrogeomorphic zone. ANOVA results are shown with superscript letters representing significant difference ($p < 0.05$) for a specific analyte among the two-way interactions of hydrogeomorphic zones and seasons using Tukey's HSD test

	Spring			Summer		
	Subtidal	Intertidal	Supratidal	Subtidal	Intertidal	Supratidal
Bulk density (g cm^{-3})	0.9^{a}	0.9^{a}	0.6^{a}	1.0^{a}	0.8^{a}	0.6^{a}
Sediment organic matter (%)	5.9^{b}	6.6^{b}	12.4^{a}	5.3^{b}	6.3^{b}	14.4^{a}
O_2 (g O_2 m^{-2} d^{-1})	$-\ 0.8^{a}$	$-\ 0.7^{a}$	$-\ 1.2^{bc}$	$-\ 1.4^{c}$	$-\ 1.3^{c}$	$-\ 2.6^{d}$
N_2–N (μmol N m^{-2} h^{-1})	34.8^{c}	50.0^{c}	296.2^{b}	315.2^{b}	322.3^{b}	734.4^{a}
NO_3^- (μmol m^{-2} h^{-1})	$-\ 15.0^{a}$	$-\ 74.9^{ab}$	$-\ 84.3^{ab}$	$-\ 204.0^{ab}$	$-\ 235.3^{b}$	$-\ 916.4^{c}$
NO_2^- (μmol m^{-2} h^{-1})	0.8^{cd}	5.0^{cd}	$-\ 2.9^{d}$	13.0^{bc}	18.3^{ab}	32.6^{a}
NH_4^+ (μmol m^{-2} h^{-1})	42.2^{b}	52.5^{b}	$-\ 31.5^{c}$	64.0^{ab}	96.3^{a}	33.7^{b}
PO_4^{3-} (μmol m^{-2} h^{-1})	2.0^{a}	$-\ 0.3^{a}$	$-\ 0.8^{ab}$	$-\ 7.5^{b}$	$-\ 0.1^{a}$	4.2^{a}

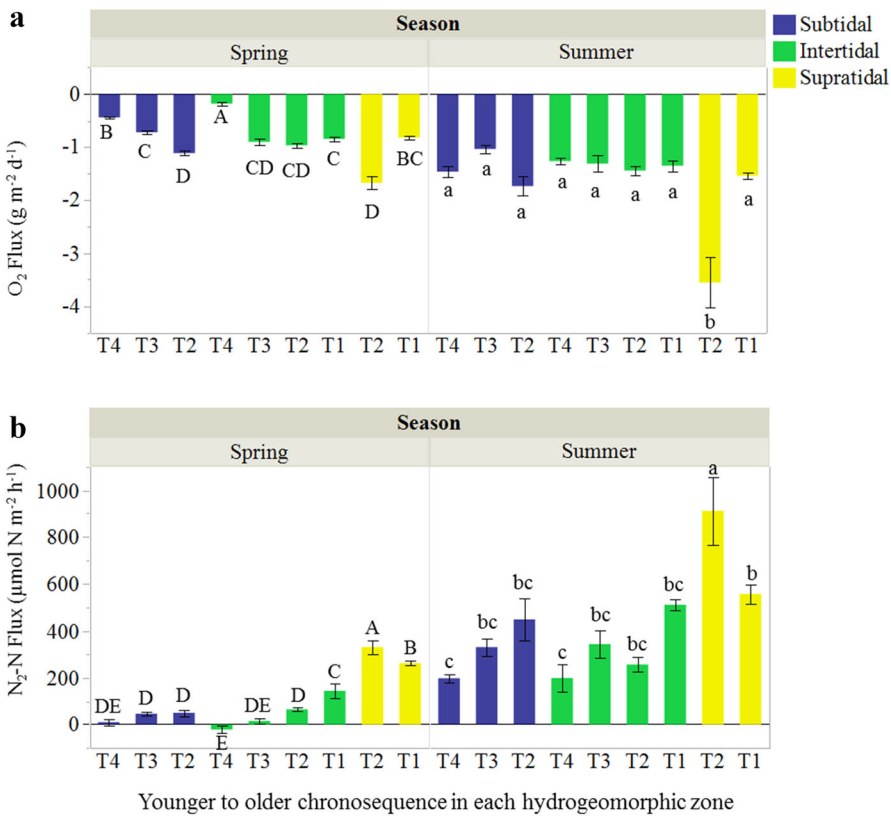

Fig. 3 Benthic fluxes of **a** dissolved oxygen and **b** N_2-N among hydrogeomorphic zones (subtidal, intertidal, and supratidal) along a chronosequence of younger (T4) to older (T1) sites within each hydrogeomorphic zone in the spring and summer (mean ± 1 SE, n = 09). ANOVA with repeated measures was used to test the difference among experimental sites in each season and letters designate significant ($p < 0.05$) differences using Tukey's HSD test

which further increases elevation (White 1993; Callaway et al. 1997; Cahoon et al. 2011; Bevington and Twilley 2018). Sediment organic matter content alters the sediment compressibility and decreases sediment bulk density (Ruehlmann and Körschens 2009). As such, bulk density decreased along the chronosequence within a hydrogeomorphic zone and from the subtidal to the supratidal zones of this coastal deltaic floodplain.

Table 4 Laboratory incubation conditions in continuous flow-through experiments in WLD. Note that the pre-filtered incubation water was collected from Wax Lake Outlet (WLO)

Variable	Spring								
	Subtidal			Intertidal				Supratidal	
	T4[b]	T3[b]	T2[b]	T4[c]	T3[c]	T2[c]	T1[a]	T2[a]	T1[a]
Temp (°C)	13.1	13.1	13.1	11.0	11.0	11.0	12.3	12.3	12.3
Salinity	0.0	0.0	0.0	0.0	0.0	0.0	0.0	0.0	0.0
NO_3^- (μM)	39.5	39.5	39.5	48.7	48.7	48.7	71.9	71.9	71.9
NO_2^- (μM)	1.4	1.4	1.4	0.6	0.6	0.6	0.7	0.7	0.7
NH_4^+ (μM)	2.8	2.8	2.8	1.2	1.2	1.2	4.0	4.0	4.0
PO_4^{3-} (μM)	1.1	1.1	1.1	1.2	1.2	1.2	1.6	1.6	1.6
Variable	Summer								
	Subtidal			Intertidal				Supratidal	
	T4[f]	T3[f]	T2[e]	T4[e]	T3[f]	T2[e]	T1[d]	T2[d]	T1[g]
Temp (°C)	22.0	22.0	22.0	22.0	22.0	22.0	22.0	22.0	22.0
Salinity	0.0	0.0	0.0	0.0	0.0	0.0	0.0	0.0	0.0
NO_3^- (μM)	67.5	67.5	90.4	90.4	67.5	90.4	105.5	105.5	101.9
NO_2^- (μM)	0.2	0.2	0.1	0.1	0.2	0.1	0.8	0.8	0.0
NH_4^+ (μM)	1.0	1.0	0.3	0.3	1.0	0.3	0.9	0.9	0.5
PO_4^{3-} (μM)	2.4	2.4	0.5	0.5	2.4	0.5	0.3	0.3	0.7

Surface sediments in the supratidal-T1 site with much lower sediment organic matter content and higher bulk density than the supratidal-T2 site indicated an alternative rather than chronosequence controlling sediment development. The supratidal-T1 site was located near the fringe along a primary channel of WLD with tree vegetation. This site was exposed to high sedimentation associated with flood pulses of inorganic sediments during river flood events (Bevington 2016; Bevington and Twilley 2018). The supratidal-T2 site, unlike the supratidal-T1, was located within the interior of the island dominated by the herbaceous community of *Colocasia esculenta*. Thus, while the supratidal-T1 and T2 sites may represent older chronosequence with higher elevation, the differences in organic matter content and bulk density between these two sites may be related to levee vs. interior location and exposure to sedimentation during a flood event. As such, chronosequence is an important factor to explain sediment organic matter content during the earlier development stages of an active deltaic floodplain, but sediment organic matter content in the supratidal zone may also depend on locations along the fringe (exposed to high mineral sedimentation) compared to interior locations (less mineral sedimentation).

The significantly increasing trend in organic matter content from younger to older chronosequences explained general patterns in benthic nutrient fluxes. There is evidence in estuarine systems that elevated sediment organic matter content enhances denitrification in wetland sediments along with increased rates of sediment oxygen demand and N mineralization (Eyre and Ferguson 2009; Hardison et al. 2015). Elevated benthic metabolism in sediments with greater organic matter content decreases dissolved oxygen concentrations in wetland sediments, providing a suitable condition for denitrification (Caffrey et al. 1993; Cai and Sayles 1996; Cornwell et al. 1999; Eyre and Ferguson 2009). Both benthic N_2 and NO_3^- fluxes increased with sediment organic matter content in our study, which are consistent with previous research results of the correlation between N_2 (NO_3^-) fluxes and sediment organic matter in WLD (Henry and Twilley 2014; their data were added in Fig. 6 as filled diamonds). The positive linear correlation between N_2 fluxes and sediment organic matter content indicates that denitrification potential is stimulated by increased sediment organic matter content as a

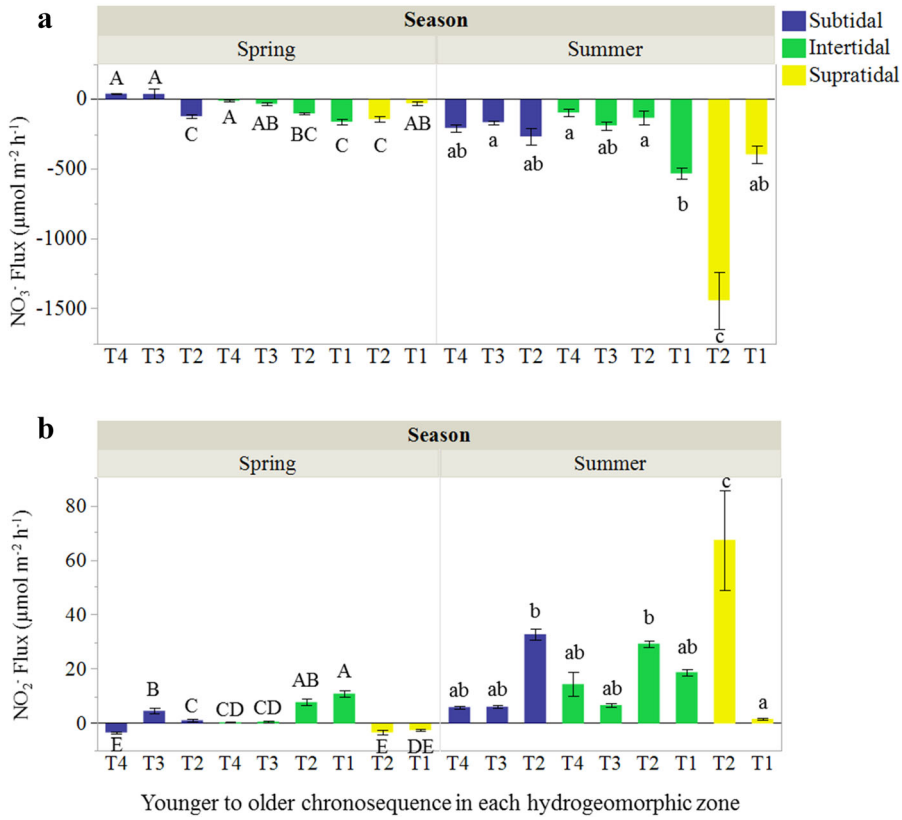

Fig. 4 Benthic fluxes of **a** NO_3^- and **b** NO_2^- among hydrogeomorphic zones (subtidal, intertidal, and supratidal) along a chronosequence of younger (T4) to older (T1) sites within each hydrogeomorphic zone in the spring and summer (mean ± 1 SE, n = 09). ANOVA with repeated measures was used to test the difference among experimental sites in each season and letters designate significant ($p < 0.05$) differences using Tukey's HSD test

function of biotic feedback associated with active deltaic succession. NO_3^- is an important electron acceptor for organic matter respiration under anaerobic conditions, and thus NO_3^- removal is positively associated with organic matter content in mostly inundated wetland soils that are anaerobic.

Sediment oxygen demand and benthic fluxes of N_2–N and NO_3^- were significantly higher in summer than in spring demonstrating the effect of temperature in this warm temperate delta in stimulating benthic biogeochemical processes (Eyre and Ferguson 2005; Giblin et al. 2010). In our experiments NO_3^- removal and N_2–N production were more sensitive to sediment organic matter content in summer than in spring, which may relate to a combination of higher NO_3^- concentrations and temperature in influent riverine waters in the summer than in the spring. Denitrification rates were enhanced at warmer temperature as increasing temperature stimulates benthic microbial activity including denitrifying bacteria (Dawson and Murphy 1972). Also, increased microbial metabolism at higher temperature reduced benthic dissolved O_2 concentrations and created a favorable condition for the anaerobic process of denitrification (Dawson and Murphy 1972; Cornwell et al. 1999). On the other hand, a pulse of riverine discharge from snowmelt and rainfall usually occurs in late winter and early spring in WLD, followed by higher NO_3^- concentrations in river waters from March to July resulting from agricultural fertilization (Xu 2006; Shaw et al. 2013; Carle et al. 2015). Influent NO_3^- concentrations were positively correlated with benthic NO_3^- fluxes (Fig. 11), which supports previous research results that sediment NO_3^- fluxes and denitrification rates are proportional to NO_3^- concentrations in overlying waters (Ogilvie et al. 1997; Kana et al. 1998; Piña-Ochoa and Álvarez-Cobelas 2006; Scaroni et al. 2011).

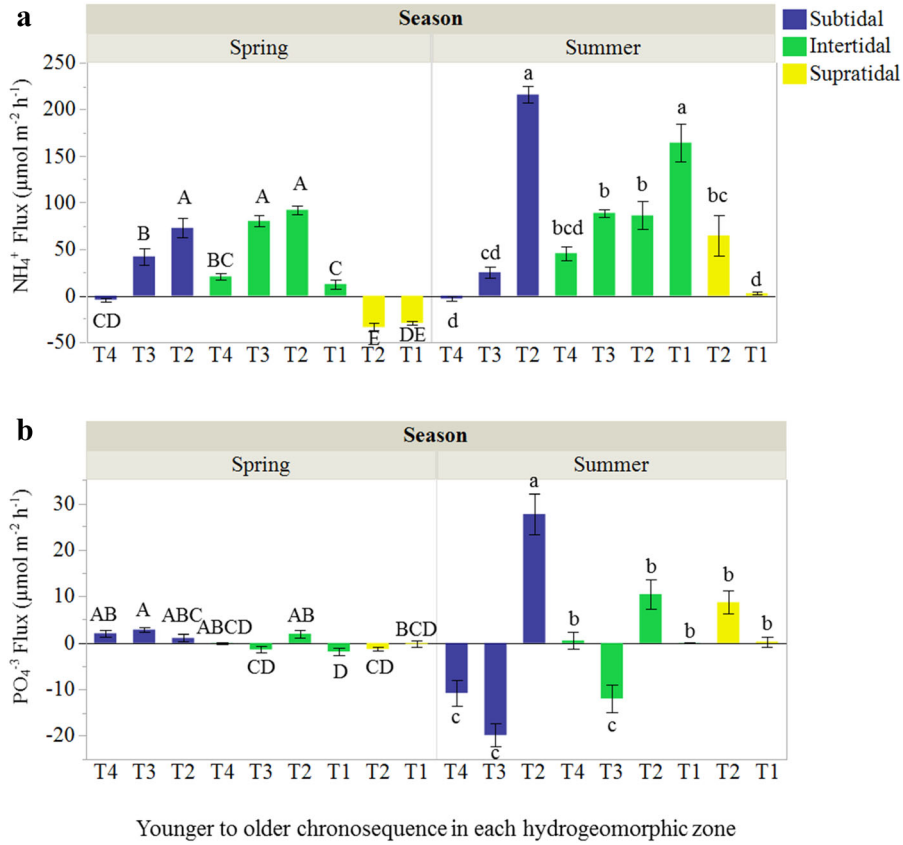

Fig. 5 Benthic fluxes of **a** NH_4^+ and **b** PO_4^{3-} among hydrogeomorphic zones (subtidal, intertidal, and supratidal) along a chronosequence of younger (T4) to older (T1) sites within each hydrogeomorphic zone in the spring and summer (mean ± 1 SE, n = 09). ANOVA with repeated measures was used to test the difference and letters designate significant ($p < 0.05$) differences among nine study sites using Tukey's HSD test

N reactions in response to benthic fluxes

N_2 production, measured here using the N_2:Ar method, represents a combination of processes that produce N_2 [anaerobic ammonium oxidation (anammox) and denitrification] and a process that consumes N_2 (N_2 fixation). Anammox is an anaerobic reaction dependent on a supply of both NH_4^+ and NO_x^- ($NO_2^- + NO_3^-$) whereas denitrification requires only NO_x^- as a N substrate (Damashek and Francis 2018). In most freshwater and estuarine ecosystems, high NO_3^- loading stimulates denitrification directly. The dominance of denitrification suppresses anammox by competition for NO_x^-, which makes anammox insignificant compared to denitrification (Wang et al. 2012; Yin et al. 2014; Damashek and Francis 2018). With relatively higher NO_3^- concentrations and lower NH_4^+ concentrations in the overlying water, WLD is expected to have much lower rates of anammox compared to denitrification as found in other similar tidal freshwater ecosystems (Trimmer et al. 2003; Koop-Jakobsen and Giblin 2009; Brin et al. 2014). However, N_2 fixation is becoming more evident as a significant process in estuarine and coastal ecosystems (Gardner et al. 2006; Yin et al. 2014; Bentzon-Tilia et al. 2015; Damashek and Francis 2018). Previous estimates of N_2 fixation in WLD sediments using the N_2:Ar method with a batch core incubation system observed that N_2 fixation exceeded denitrification when overlying NO_3^- concentration was low (about 2.0 µM; Henry and Twilley 2014). Nevertheless, our experiments were under eutrophic NO_3^- concentrations (39.5 to 105.5 µM) and showed mainly positive N_2–N production without obvious evidence of net N_2 fixation. Several studies have also reported that bioreactive N at high concentrations (≥ 10 µM) could

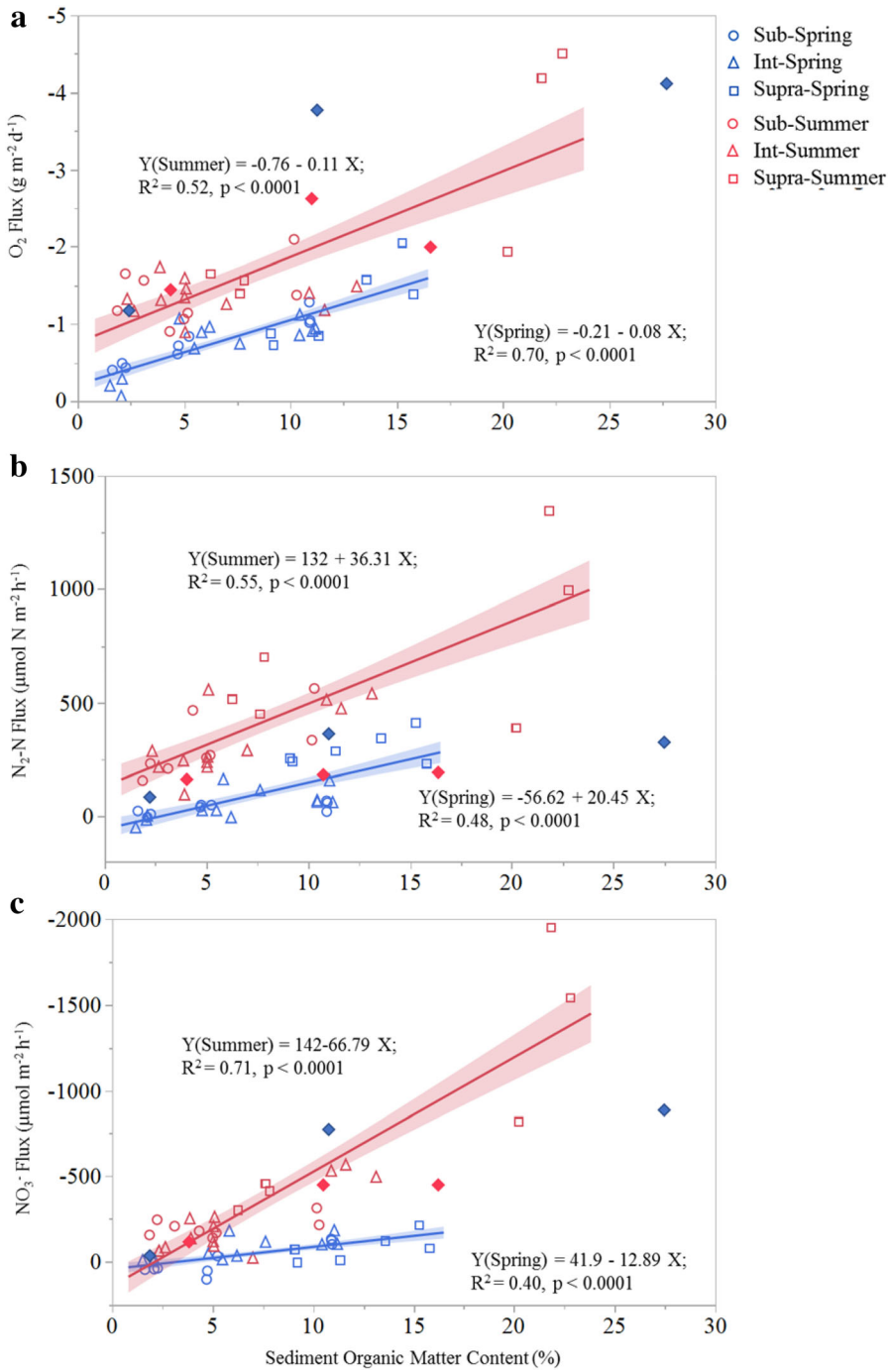

Fig. 6 Benthic fluxes of **a** dissolved oxygen, **b** N_2–N and **c** NO_3^- as functions of sediment organic matter content in Wax Lake Delta (WLD). Note each data point represents a sediment core and values of O_2 and NO_3^- fluxes were inversed on the x-axis. Henry and Twilley 2014) data in spring and summer were added as filled diamonds in corresponding colorshowever, these values were not included in correlation models

significantly inhibit N_2 fixation (Howarth et al. 1988; Mulholland et al. 2001; Capone et al. 2008; Scott et al. 2008). Assuming this threshold of NO_3^- concentration for WLD, the N_2–N production rates measured in our study represent denitrification rates in WLD with little impact of N_2 fixation.

Incomplete denitrification to N_2O is frequently reported to be small compared to complete denitrification in riverine and coastal ecosystems (Seitzinger

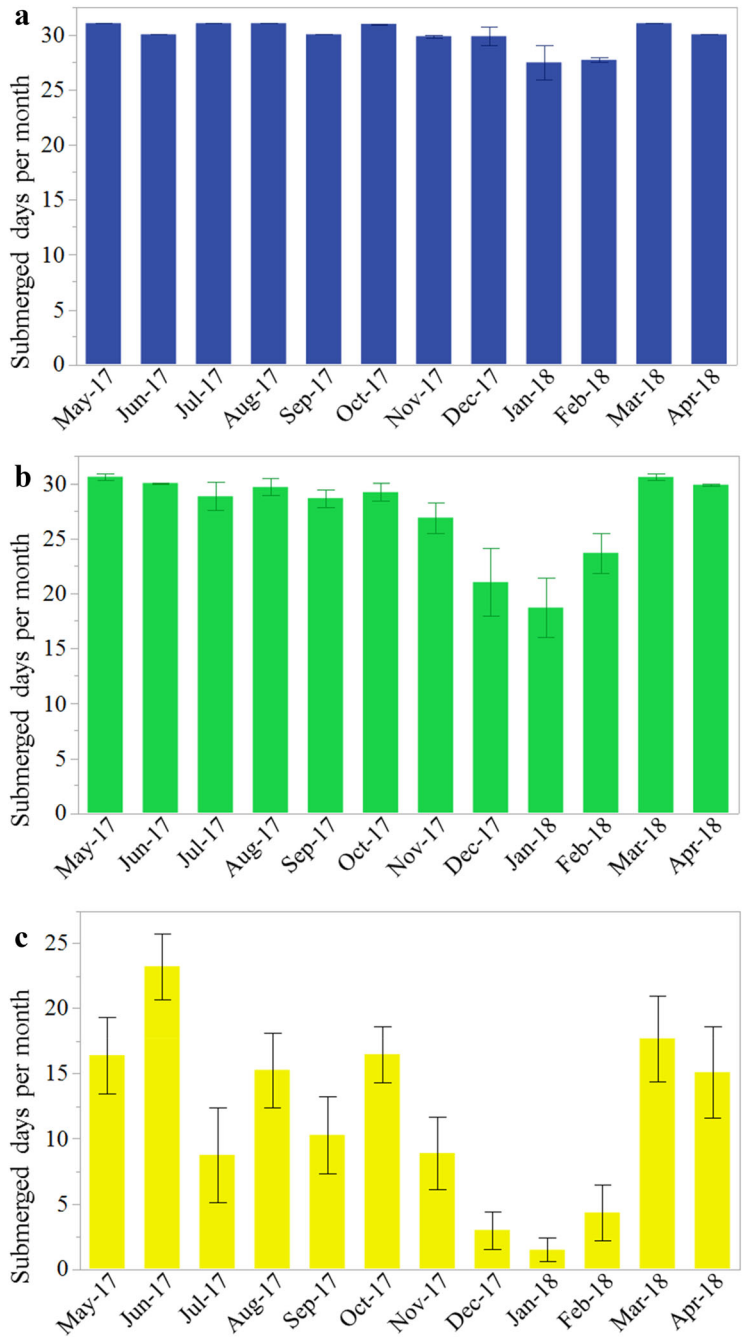

Fig. 7 Monthly flooded times for **a** subtidal, **b** intertidal and **c** supratidal hydrogeomorphic zones in Wax Lake Delta (WLD) from May 2017 to April 2018 (recognized as a sampling year). Error bars are standard errors among different chronosequence zones within each hydrogeomorphic zone. Flooded time was estimated based on the elevations of nine sites and continuous water level records at 6 min time intervals from a tidal gauge (29° 27.0′ N, 91° 20.3′ W) in Amerada Pass near WLD

et al. 1984; Yu et al. 2006; Beaulieu et al. 2011). Assuming incomplete denitrification is negligible in our research, N_2–N production rates should be balanced with NO_3^- removal rates if all N_2–N is from direct denitrification and there is little impact of N_2 fixation. However, if coupled nitrification-denitrification occurs, some atoms of N_2–N are produced from NO_3^- formed within sediments from nitrification, leading to higher N_2–N production rates compared to NO_3^- removal rates. On the other hand, when N_2–N production rates are significantly less than NO_3^- removal rates, there is evidence that some NO_3^- is not used in denitrification, but instead contributes to dissimilatory nitrate reduction to ammonium (DNRA)

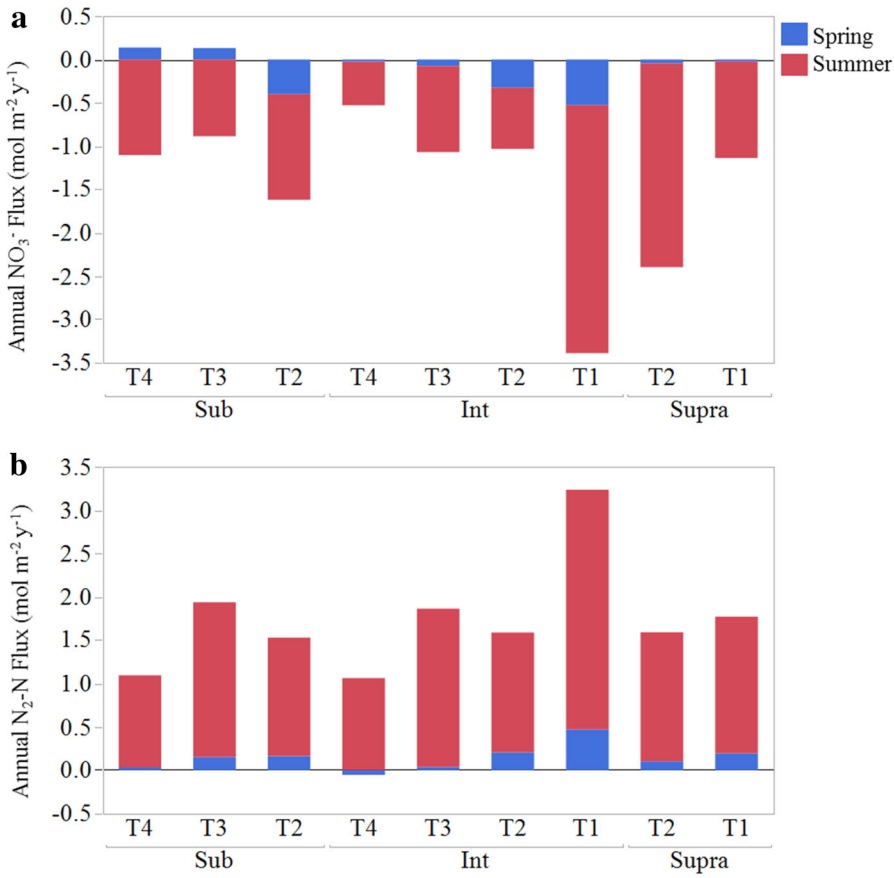

Fig. 8 Annual rates for **a** NO_3^- removal and **b** N_2–N production based on hourly NO_3^- and N_2–N fluxes at the sediment-water interface applying spring vs. summer rates based on ambient water temperature together with the amount of time that a specific hydrogeomorphic zone is inundated. The critical water temperature we used to separate months into spring/summer seasons is 17 °C

assuming incomplete denitrification is negligible. N_2–N production was higher than NO_3^- removal in the sub-T3 site and most sites in the intertidal zone, indicating coupled nitrification-denitrification was present in these sediments and outcompeted DNRA (assuming anammox and N_2 fixation are negligible; Fig. 8a and b). In contrast, N_2–N production was lower than NO_3^- removal rates in the supratidal-T2 site, indicating DNRA was more favorable than coupled nitrification-denitrification in this site. DNRA was reported to be a prominent NO_3^- reduction pathway in estuarine and coastal ecosystems, especially under high organic carbon content (An and Gardner 2002; Koop-Jakobsen and Giblin 2010; Giblin et al. 2013; Hardison et al. 2015). It is reasonable that the supratidal-T2 site had higher DNRA rates because of the significantly higher organic matter content (18.2%) in this site compared to other sites in WLD. However, these estimates should be treated with some caution since N cycles are more complex than the methodologies used in this study to discern specific transformations of N in delta sediments.

Stoichiometry of benthic fluxes

Denitrification can be estimated based on stoichiometric ratios of dissolved oxygen and inorganic N assuming constant ratios of elements related to the dominant terminal electron acceptors in eutrophic coastal sediments (Boynton and Kemp 1985; Cowan et al. 1996; Cornwell et al. 1999; Boynton et al. 2018):

$$(CH_2O)_{106}(NH_3)_{16}H_3PO_4 + 138O_2 \rightarrow 106CO_2 + 16HNO_3 + H_3PO_4 + 122H_2O \quad (2)$$

Every 17.25 atoms of dissolved oxygen consumed in sediments should result in 1 atom of DIN released to porewater and then diffused across the sediment-water interface to the overlying water to reach an equilibrium (Redfield 1934; Boynton and Kemp 1985). Dissolved oxygen consumption we measured in the flow-through system was presumed to represent

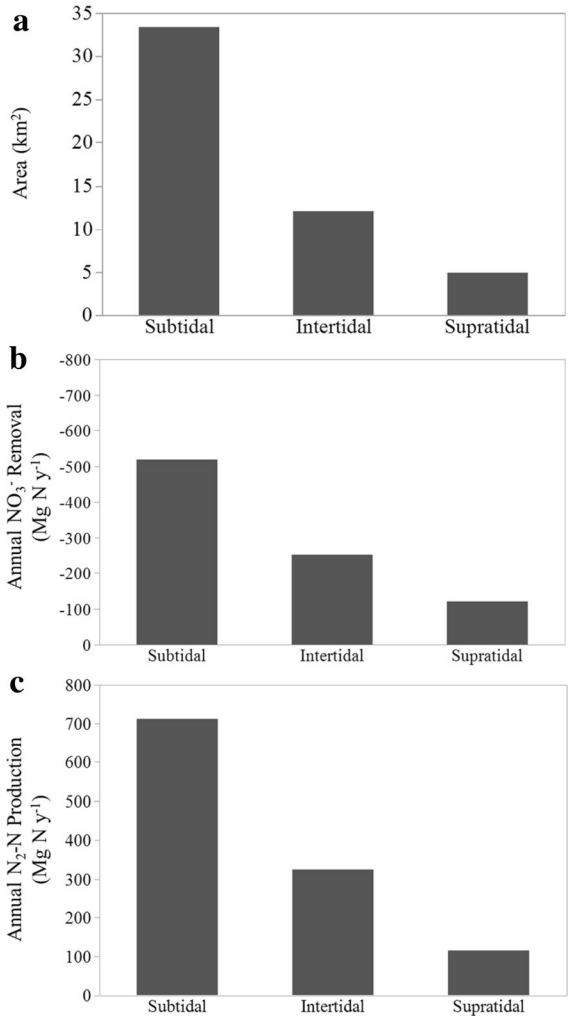

Fig. 9 Using **a** the area of each hydrogeomorphic zone at Wax Lake Delta and per unit area rates of nitrogen fluxes to estimate **b** annual NO_3^- removal and **c** N_2–N production in each hydrogeomorphic zone

sediment oxygen demand (the benthic consumption of O_2 due to aerobic respiration as shown in EQ 2) since our incubations occurred in the dark and the overlying water was filtered before use. We assumed that the C:O:N ratio of sediment organic matter in WLD followed the Redfield composition. Multiplying the measured rates of sediment oxygen demand by the Redfield ratio of 17.25 provided expected DIN fluxes across the sediment-water interface. The expected DIN fluxes were different from measured DIN fluxes, which is reasonable since denitrification occurred and converted DIN to N_2 gas during the incubations. As such, the measured DIN fluxes are combinations of the expected DIN production from benthic aerobic respiration following Redfield ratio and the DIN uptake due to denitrification.

Denitrification rates can be indirectly estimated by subtracting the measured DIN fluxes with the expected DIN fluxes (Cowan and Boynton 1996). Estimated denitrification rates calculated indirectly based on the stochiometric ratio were significantly correlated to measured net denitrification rates from the N_2:Ar method (Fig. 12; $R^2 = 0.73$ and $p < 0.0001$). However, the slope of estimated denitrification to measured denitrification rates was significantly higher than one (slope = 1.27, $p < 0.01$), indicating that the estimated denitrification rates using the stoichiometric ratio of 17.25 were higher than the measured denitrification rates. An implicit assumption with using this stoichiometric ratio to estimate denitrification is that the sediment organic matter has the Redfield composition of C:O:N ratio (Cornwell et al. 1999). Nevertheless, the Redfield ratio (C:O:N:P = 106:138:16:1) is an average ratio of phytoplankton biomass composition (Redfield 1934, 1958; Hillebrand and Sommer 1999). Previous research showed that this ratio had significant local variations, which could depart broadly from the average due to different nutrient availabilities and planktonic species (Geider and La Roche 2002; Ptacnik et al. 2010). WLD is mainly N limited with low C:N (9.7 to 11.6) and N:P ratios (Henry and Twilley 2014), which may result in a lower stochiometric ratio than 17.25 and an overestimate of denitrification using the ratio of 17.25. Stoichiometry of benthic fluxes is a complex balance between several biological processes rather than a fixed ratio, and thus rates based on the Redfield ratio should be treated with caution (Geider and La Roche 2002).

Another explanation for higher estimated denitrification than measured denitrification is that the N_2:Ar method may underestimate denitrification because of the occurrence of N_2 fixation, incomplete denitrification and/or gas bubbles during the incubation (Eyre and Ferguson 2002; Ferguson and Eyre 2007; Henry and Twilley 2014). As discussed, N_2 fixation and incomplete denitrification are reported to be small compared to total denitrification in eutrophicated coastal wetlands, rivers and coastal bays (Seitzinger et al. 1984; Howarth et al. 1988; Mulholland et al. 2001; Yu et al. 2006; Capone et al. 2008; Scott et al. 2008). Also, our incubations were completed in the dark using pre-filtered overlying water and were

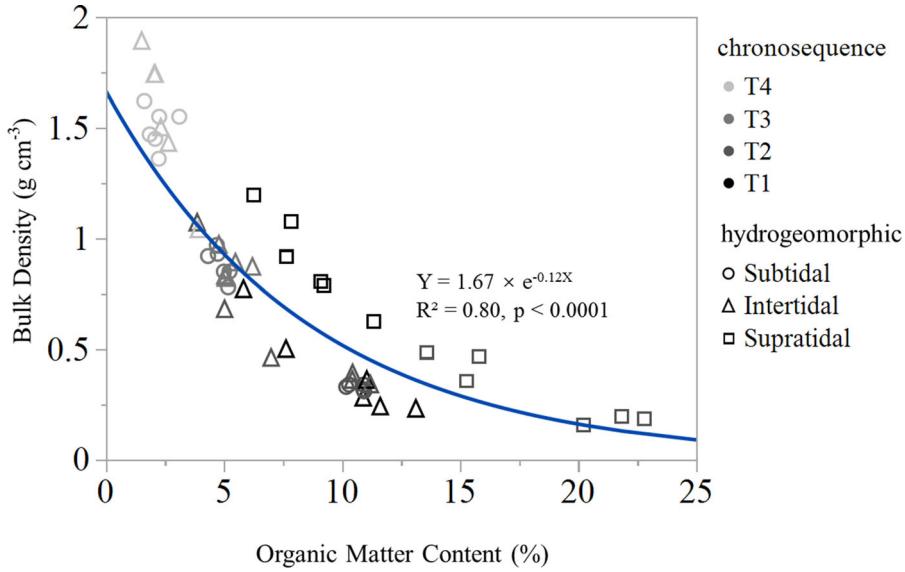

Fig. 10 Bulk density as a function of sediment organic matter content in Wax Lake Delta (WLD). Note each data point represents a sediment core

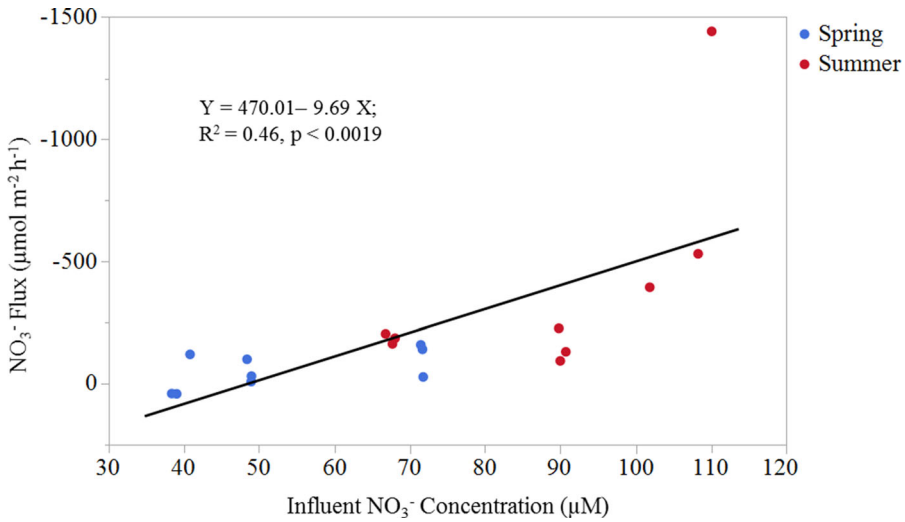

Fig. 11 Correlation between NO_3^- fluxes versus influent NO_3^- concentrations during incubations. Note that each data point represents an averaged value in each site

closely monitored for the occurrence of bubbles. The influence of gas bubbles to the measured net denitrification should be small.

Are coastal deltas hotspots of N removal?

The sediment organic matter content and hydroperiod of each hydrogeomorphic zone are important factors to determine annual benthic fluxes of a coastal deltaic floodplain. Organic matter determines benthic flux per unit time of inundation, and hydroperiod defines the duration that an area of sediment is inundated with overlying water (and NO_3^-). The intertidal and supratidal zones are submerged seasonally, with less hours per month during late fall and early winter seasons when river stage and frequency of cold fronts are the lowest (Bevington 2016; Twilley et al. 2019). Annual estimates of N removal for intertidal and

supratidal sites account for both seasonal water temperature and flood duration. For subtidal sediments, water temperature is a key factor since these sites are inundated nearly all year. Considering these seasonal and hydroperiod factors among sites representing subtidal, intertidal and supratidal hydrogeomorphic zones, our annual benthic NO_3^- fluxes varied from − 0.5 to − 3.4 mol N m^{-2} y^{-1}. The upper range of NO_3^- removal at WLD are comparable to a recent estimate in the Mississippi River Basin based on a mass balance calculation (average = − 3.3 mol N m^{-2} y^{-1}; Mitsch et al. 2005). Annual N_2–N production rates varied from 1.0 to 3.2 mol N m^{-2} y^{-1}, which is comparable to annual NO_3^- removal.

Total NO_3^- load to WLD can be calculated by multiplying the estimated NO_3^- loading rate of 66 to 172 g N m^{-2} y^{-1} in the Atchafalaya River estuarine complex (Lane et al. 2002) with the area of WLD (50 km^2). Based on this calculation, WLD could receive 3300 to 8600 Mg N y^{-1}. The estimated annual NO_3^- removal of 896 Mg N y^{-1} in WLD accounts for 10 to 27% of total NO_3^- load to WLD, most of which is converted to N_2 gas since NO_3^- removal rate is comparable to N_2–N production in our study. Over 90% of the annual NO_3^- removal occurred during warmer temperatures (≥ 17 °C) when higher NO_3^- concentrations due to agricultural fertilization were present in the overlying water. As such, coastal deltaic floodplains like WLD play an important role in decreasing nutrient concentrations in warm seasons before nutrient enriched water enters the Gulf of Mexico (Henry and Twilley 2014).

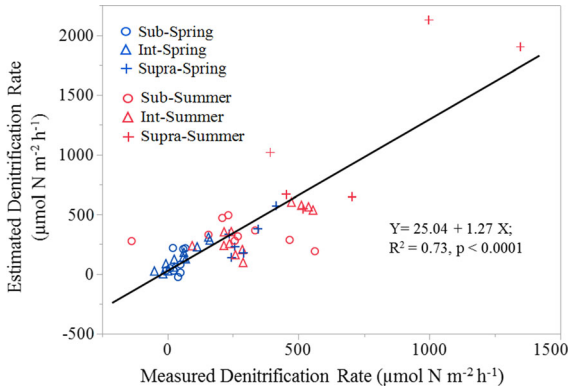

Fig. 12 Correlation between direct measurements of benthic denitrification using the N_2:Ar method versus estimated denitrification rates based on the stoichiometric assumption that the molar organic carbon (C):oxygen (O):nitrogen (N):phosphorus (P) ratios of sediment fluxes should follow Redfield composition (C:O:N:P = 106:138:16:1). Note that each data point represents a sediment core in each site

Active deltas, such as WLD, have the unique landscape feature of annual progradation as young subtidal hydrogeomorphic zones, which increases the N removal capacity. For example, WLD with a land growth rate of 1.0 to 5.0 km^2 y^{-1} (Allen et al. 2012; Shaw et al. 2013; Bevington 2016) increases the capacity of NO_3^- removal by 14 to 70 Mg N per year (0.2 to 2% of total NO_3^- load) as a result of continuous delta progradation. In addition to annual delta growth, there is a shift in proportion of hydrogeomorphic zones from subtidal to intertidal and supratidal zones in response to organic matter accumulation and infilling as emergent vegetation expands with increased sediment elevation (Bevington and Twilley 2018; Ma et al. 2018; Twilley et al. 2019). Increasing areas of intertidal and supratidal zones favor N removal in WLD as denitrification rates are higher with higher sediment organic matter. The expansion of the intertidal zone may contribute more to benthic N removal after years of organic matter accumulation as this area is inundated more frequently compared to the supratidal zone. Active delta formation at the mouth of rivers that have waters enriched with NO_3^- is a dynamic process in reducing eutrophication of the coastal ocean. Mineral sedimentation stimulates delta formation during winter and spring flood-pulse of the river (Bevington and Twilley 2018) whereas the warmer growing season of wetlands contribute organic production in summer and fall (Aarons 2019). The combination of both processes contributes to the formation of depositional landscapes that increases N removal capacity in active deltaic basins with connectivity between channels and hydrogeomorphic zones (Hiatt et al. 2018).

Our estimates of NO_3^- removal and N_2 production are conservative for several reasons. Firstly, subtidal zones with elevation lower than − 0.75 m and all creeks and channels are excluded as part of the total subtidal area estimate for WLD. These regions account for about 40% of total WLD, and their benthic biogeochemical processes may be different from our experimental sites due to distinct environmental conditions (sediment organic matter content, water residence time, water temperature). Denitrification that occurs in these regions is not included in our analysis of NO_3^- removal. Secondly, our estimates

focus on the hydroperiod of wetland submergence that determines NO_3^- removal when river waters are in contact with deltaic sediments. The emergence of deltaic sediments in intertidal and supratidal hydrogeomorphic zones may prompt nitrification that is later denitrified when sediments are submerged (Cornwell et al. 1999; Baldwin and Mitchell 2002; Pinay et al. 2002). Partial drying of previously submerged sediments will produce a zone for coupled nitrification-denitrification (Patrick and Reddy 1976; Baldwin and Mitchell 2002). Coupled nitrification-denitrification rates may be enhanced by seasonal hydroperiod from emergence to submergence in more elevated hydrogeomorphic zones. Since our focus is on estimates of riverine NO_3^- removal in coastal deltaic floodplains, this coupled process of nitrification as a source of NO_3^- may not be relevant to our analysis, but could impact the total N_2 flux from active deltaic floodplains to the atmosphere.

Our estimate of N removal at the sediment-water interface may not account for field boundary conditions at the sediment-water interface as result of flow currents that can impact benthic fluxes. This may be particularly important at the subtidal zone in the younger chronosequences (T4 and T3), where more open water with strong hydrological connectivity may present different conditions than found in our incubation system (Hiatt and Passalacqua 2015). Additionally, dark incubations reflect limited diurnal variability of benthic fluxes compared to field conditions. Benthic fluxes in WLD are reported to have diurnal variability in the field because of the photosynthesis of benthic microalgae in light condition (Henry 2012). In the light, experimental sites with benthic microalgae could have higher benthic NO_3^- and NH_4^+ uptakes, lower dissolved O_2 consumption and lower denitrification rates compared to the dark incubations (Sundback et al. 1991; Henry 2012). In addition, two temperature settings simplified the seasonal variability of benthic fluxes, but our incubations at 12 and 22 °C did mirror environmental conditions as these two temperatures are representative temperatures for cold (winter and spring) and warm (summer and fall) seasons that provide a first approximation of seasonal temperature variation. Surface water temperatures in WLD fell within 12 to 22 °C for about half time of the year. Also, the supratidal and intertidal zones tend to have higher water temperature than the subtidal zone because longer water residence time in supratidal and intertidal zones allows water temperatures to increase from solar radiation (Christensen 2017; Noe et al. 2013). Applying water temperature records from the intertidal zone to subtidal and supratidal hydrogeomorphic zones may weaken hydrogeomorphic variations in annual N removal. Model simulation of benthic N processes and field experiments that include physical conditions like hydrological connectivity and currents may expand our understanding of these additional factors that control NO_3^- removal in coastal deltaic floodplains (Christensen 2017).

Our analysis demonstrates the importance of active deltaic floodplains in N removal as these landscapes become subaerially emergent before significant N enters the coastal ocean. The potential capacity of N removal can be further demonstrated by applying the N removal capacity in WLD to the Atchafalaya River Coastal Basin (ARB). ARB is about 4678 km^2 in area with over 150 km^2 of newly emergent delta including WLD in Atchafalaya Bay (Coleman et al. 1998; Xu 2006). Annual NO_3^- loading to ARB is about 170,000 Mg (Xu 2006). Assuming the N removal capacity in WLD is similar to the capacity in wetland landscapes across ARB, about 50% of riverine NO_3^- could be removed before entering the Gulf of Mexico. Though the N removal capacity of 50% in ARB may be underestimated as describe above, it is consistent with the conclusion that ARB removes 41 to 47% of NO_3^- from the Atchafalaya River (Lane et al. 2002). With increasing coastal water temperature due to global climate change, the role of coastal deltaic floodplain in benthic N removal may be enhanced since warmer temperature increases benthic denitrification rates (Dawson and Murphy 1972; Michener et al. 1997). Our study provides new insights into how active deltaic floodplains may remove riverine N as part of delta restoration efforts. We propose that the extension of older intertidal zone as the most efficient N-removal area, annual progradation of younger subtidal areas, vegetative production that elevates SOM concentrations and frequent riverine water inundation all lead to higher N removal capacity of a newly restored delta.

The combined effects of anthropogenic changes to sediment supply and river connectivity to coastal deltaic floodplains as result of river abandonment, along with subsidence and sea level rise, are causing river deltas all over the world to decrease in emergent area along deltaic coasts (Syvitski et al. 2009;

Vörösmarty et al. 2009; Twilley et al. 2016). The Mississippi River Delta Plain covers an area of 30,000 km^2 (Coleman et al. 1998), which represents coastal deltaic floodplains with potential to remove N before riverine nutrients reach the ocean. However, anthropogenic modifications, such as the construction of levees and flood-control structures along the Mississippi River, convert this once active delta into an inactive floodplain that is abandoned from connectivity with riverine waters (Twilley et al. 2016). These inactive deltaic floodplains no longer contribute to riverine N removal that could potentially reduce coastal eutrophication on the Louisiana Bight (Diaz and Rosenberg 2008; Bargu et al. 2019; Twilley et al. 2019; White et al. 2019). Reconnecting the previously isolated coastal deltaic floodplains to river flood pulse is proposed as a feasible way to not only restore coastal wetland habitats, but also re-build ecosystems for processing polluted riverine water (Mitsch et al. 2005; Bargu et al. 2019; Twilley et al. 2019; White et al. 2019). Scaling the capacity of an active deltaic floodplain such as WLD, accounting for both chronosequence and hydrogeomorphic zones as influential factors in N removal, can serve as a model of how riverine nutrients will be processed under the ecological succession of a young emergent delta created from major river diversions.

Conclusions

We investigated spatial and seasonal patterns in benthic fluxes and estimated annual N removal in the newly emergent WLD using continuous flow-through incubations of intact sediment cores. To our knowledge, it is the first assessment on benthic fluxes as a function of hydrogeomorphology and delta age since emergence in coastal deltaic floodplains. This study suggests that benthic fluxes have obvious variations within different hydrogeomorphic zones and chronosequence zones in response to the change in sediment organic matter content. Denitrification rates estimated from the stochiometric ratio of C:O:N (106:138:16) explained 73% of the measured net denitrification rates using the N_2:Ar method. But the use of stoichiometry in benthic denitrification calculation should be used with caution as the Redfield ratio is a complex balance between several biological processes rather than a fixed ratio. The older intertidal hydrogeomorphic zones with relatively higher sediment organic matter was the most efficient site in annual N removal. Subtidal zone had the lowest denitrification rates associated with lower organic matter content, but was the largest hydrogeomorphic zone with the longest flood duration, and therefore contributed over half of the N removal in WLD. The estimated annual NO_3^- removal of 896 Mg N y^{-1} in WLD accounted for 10 to 27% of total NO_3^- load to WLD, most of which was converted to N_2 gas. Over 90% of the annual N removal occurred during warmer temperatures ($\geq$ 17 °C) when higher NO_3^- concentrations were observed in the overlying water. WLD is a continuously emerging ecosystem where the capacity for N removal increases by 0.2–2% per year prior to riverine NO_3^- is export to coastal ocean.

We conclude that coastal deltaic floodplains play an important role in decreasing nutrient concentrations before riverine water entering the Gulf of Mexico. The capacity for N removal in active coastal deltaic floodplains like WLD increases with continuously emerging ecosystems at continental margins. This research of nutrient cycling in WLD concerning chronosequence and hydrogeomorphic zones as influential factors provides a basic understanding of how riverine nutrients will be processed under the ecological succession of a young emergent delta created from major river diversions. Further analysis of model simulation incorporating actual hydrological connectivity, water residence time and the growth of an active delta with newly emergent subtidal hydrogeomorphic zones and continued development of intertidal to supratidal zones will more clearly define the role of coastal deltaic floodplains in processing elevated riverine NO_3^- in major river basin.

Acknowledgements This work was supported by the National Science Foundation via the Coastal SEES program at LSU [EAR-1427389]. This manuscript was prepared under award R/MMR-33 to Louisiana Sea Grant College Program by NOAA's Office of Ocean and Atmospheric Research, U.S. Department of Commerce. We would like to thank Thomas Blanchard for assistance on analytical techniques, Kanchan Maiti, John White, Bin Li and Nancy N. Rabalais for helpful suggestions. We appreciate the editor and two anonymous reviewers for constructive comments.

References

Aarons AA (2019) Spatial and temporal patterns of ecological succession and land development along a coastal deltaic floodplain chronosequence. Dissertation, Louisiana State University

Allen YC, Couvillion BR, Barras JA (2012) Using multitemporal remote sensing imagery and inundation measures to improve land change estimates in coastal wetlands. Estuar Coasts 35:190–200. https://doi.org/10.1007/s12237-011-9437-z

An S, Gardner WS (2002) Dissimilatory nitrate reduction to ammonium (DNRA) as a nitrogen link, versus denitrification as a sink in a shallow estuary (Laguna Madre/Baffin Bay, Texas). Mar Ecol Prog Ser 237:41–50. doi:https://doi.org/10.3354/meps237041

Baldwin DS, Mitchell AM (2002) The effects of drying and reflooding on the sediment and soil nutrient dynamics of lowland river–floodplain systems: a synthesis. Regul Riv Res Manag 16:457–467.

Bargu S, Justic D, White JR, Lane R, Day J, Paerl H, Raynie R (2019) Mississippi River diversions and phytoplankton dynamics in deltaic Gulf of Mexico estuaries: a review. Estuar Coast Shelf Sci. https://doi.org/10.1016/j.ecss.2019.02.020

Bentzon-Tilia M, Traving SJ, Mantikci M, Knudsen-Leerbeck H, Hansen JL, Markager S, Riemann L (2015) Significant N_2 fixation by heterotrophs, photoheterotrophs and heterocystous cyanobacteria in two temperate estuaries. ISME J 9:273–285. doi:https://doi.org/10.1038/ismej.2014.119

Bevington AE (2016) Dynamics of land building and ecological succession in a prograding deltaic floodplain, Wax Lake delta, LA, USA. Dissertation, Louisiana State University

Bevington AE, Twilley RR (2018) Island Edge Morphodynamics along a chronosequence in a prograding deltaic floodplain wetland. J Coast Res 344:806–817. https://doi.org/10.2112/jcoastres-d-17-00074.1

Boynton WR, Kemp W (1985) Nutrient regeneration and oxygen consumption by sediments along an estuarine salinity gradient. Mar Ecol Prog Ser 23:45–55. doi:https://doi.org/10.3354/meps023045

Boynton WR, Ceballos MAC, Bailey EM, Hodgkins CLS, Humphrey JL, Testa JM (2018) Oxygen and nutrient exchanges at the sediment-water interface: a global synthesis and critique of estuarine and coastal data. Estuar Coasts 41:301–333. https://doi.org/10.1007/s12237-017-0275-5

Brin LD, Giblin AE, Rich JJ (2014) Environmental controls of anammox and denitrification in southern New England estuarine and shelf sediments. Limnol Oceanogr 59:851–860. doi:https://doi.org/10.4319/lo.2014.59.3.0851

Bryantmason A, Xu YJ, Altabet M (2013) Isotopic signature of nitrate in river waters of the lower Mississippi and its distributary, the Atchafalaya. Hydrol Process 27:2840–2850. doi:https://doi.org/10.1002/hyp.9420

Caffrey JM, Sloth NP, Kaspar HF, Blackburn TH (1993) Effect of organic loading on nitrification and denitrification in a marine sediment microcosm. FEMS Microbiol Ecol 12:159–167. doi:https://doi.org/10.1111/j.1574-6941.1993.tb00028.x

Cahoon DR, White DA, Lynch JC (2011) Sediment infilling and wetland formation dynamics in an active crevasse splay of the Mississippi River delta. Geomorphology 131:57–68. doi:https://doi.org/10.1016/j.geomorph.2010.12.002

Cai W-J, Sayles FL (1996) Oxygen penetration dephts and fluxes in marine sediments. Mar Chem 52:123–131. doi:https://doi.org/10.1016/0304-4203(95)00081-X

Callaway JC, DeLaune RD, Patrick WH Jr (1997) Sediment accretion rates from four coastal wetlands along the Gulf of Mexico. J Coast Res 13(1):181–191

Canfield DE, Glazer AN, Falkowski PG (2010) The evolution and future of earth's nitrogen cycle. Science 330:192–196. doi:https://doi.org/10.1126/science.1186120

Capone DG, Bronk DA, Mulholland MR, Carpenter EJ (eds) (2008) Nitrogen in the marine environment. Elsevier, Amsterdam

Carle MM (2013) Spatial structure and dynamics of the plant communities in a pro-grading river delta: Wax Lake Delta, Atchafalaya Bay, Louisiana. Dissertation, Louisiana State University

Carle MV, Sasser CE, Roberts HH (2015) Accretion and vegetation community change in the Wax Lake Delta following the historic 2011 Mississippi River flood. J Coast Res 313:569–587. https://doi.org/10.2112/JCOASTRES-D-13-00109.1

Christensen A (2017) Hydrodynamic modeling of newly emergent coastal deltaic floodplains. Thesis, Louisiana State University

Clawson RG, Lockaby BG, Rummer B (2001) Changes in production and nutrient cycling across a wetness gradient within a floodplain forest. Ecosystems 4:126–138. doi:https://doi.org/10.1007/s100210000063

Coleman JM, Roberts HH, Stone GW (1998) Mississippi River delta: an overview. J Coast Res 14:3

Conley DJ, Paerl HW, Howarth RW, Boesch DF, Seitzinger SP, Havens KE, Lancelot C, Likens GE (2009) Controlling eutrophication: nitrogen and phosphorus. Science 323:1014–1015. https://doi.org/10.1126/science.1167755

Cornwell JC, Kemp WM, Kana TM (1999) Denitrification in coastal ecosystems: methods, environmental controls, and ecosystem level controls, a review. Aquat Ecol 33:41–54. doi:https://doi.org/10.1023/A:1009921414151

Cowan JLW, Boynton WR (1996) Sediment-water oxygen and nutrient exchanges along the longitudinal axis of Chesapeake Bay: seasonal patterns, controlling factors and ecological significance. Estuaries. https://doi.org/10.2307/1352518

Cowan JLW, Pennock JR, Boynton WR (1996) Seasonal and interannual patterns of sediment-water nutrient and oxygen fluxes in Mobile Bay, Alabama (USA): regulating factors and ecological significance. Mar Ecol Prog Ser 141:229–245. https://doi.org/10.3354/meps141229

Damashek J, Francis CA (2018) Microbial nitrogen cycling in estuaries: from genes to ecosystem processes. Estuaries Coasts 41:626–660. https://doi.org/10.1007/s12237-017-0306-2

Davidson EA, Seitzinger SP (2006) The enigma of progess in denitrification research. Ecol Appl 16:2057–2063. https://

doi.org/10.1890/1051-0761(2006)016[2057:TEOPID]2.0.CO;2
Dawson RN, Murphy KL (1972) The temperature dependency of biological denitrification. Water Res. doi:https://doi.org/10.1016/0043-1354(72)90174-1
Diaz RJ, Rosenberg R (2008) Spreading dead zones and consequences for marine ecosystems. Science 321:926–929. https://doi.org/10.1126/science.1156401
Eyre BD, Ferguson AJP (2002) Comparison of carbon production and decomposition, benthic nutrient fluxes and denitrification in seagrass, phytoplankton, benthic microalgae- and macroalgae-dominated warm-temperate Australian lagoons. Mar Ecol Prog Ser 229:43–59. doi:https://doi.org/10.3354/meps229043
Eyre BD, Ferguson AJP (2005) Benthic metabolism and nitrogen cycling in a subtropical east Australian estuary (Brunswick): Temporal variability and controlling factors. Limnol Oceanogr 50:81–96. doi:https://doi.org/10.4319/lo.2005.50.1.0081
Eyre BD, Ferguson AJP (2009) Denitrification efficiency for defining critical loads of carbon in shallow coastal ecosystems. Hydrobiologia 629:137–146. doi:https://doi.org/10.1007/s10750-00909765-1
Ferguson AJP, Eyre BD (2007) Seasonal discrepancies in denitrification measured by isotope pairing and N2:Ar techniques. Mar Ecol Prog Ser 350:19–27. doi:https://doi.org/10.3354/meps07152
Fixen PE, West FB (2002) Nitrogen fertilizers: meeting contemporary challenges. AMBIO 31:169–176. https://doi.org/10.1579/0044-7447-31.2.169
Gardner WS, McCarthy MJ, An S, Sobolev D (2006) Nitrogen fixation and dissimilatory nitrate reduction to ammonium (DNRA) support nitrogen dynamics in Texas estuaries. Limnol Oceanogr 51:558–568. doi:https://doi.org/10.4319/lo.2006.51.1_part_2.0558
Gardner WS, McCarthy MJ (2009) Nitrogen dynamics at the sediment-water interface in shallow, sub-tropical Florida Bay: why denitrification efficiency may decrease with increased eutrophication. Biogeochemistry 95:185–198. https://doi.org/10.1007/s10533-009-9329-5
Geider RJ, La Roche J (2002) Redfield revisited: variability of C:N:P in marine microalgae and its biochemical basis. Eur J Phycol 37:1–17. https://doi.org/10.1017/S0967026201003456
Giblin A, Hopkinson CS, Tucker J, Nowicki BL, Kelly JR (1995) Metabolism, nutrient cycling and denitrification in Boston Harbor and Massachusetts Bay sediments in 1994. Massachusetts Water Resources Authority, Environmental Quality Department
Giblin AE, Hopkinson CS, Tucker J (1997) Benthic metabolism and nutrient cycling in Boston Harbor. Mass Estuar 20:346–364. https://doi.org/10.2307/1352349
Giblin AE, Weston NB, Banta GT, Tucker J, Hopkinson CS (2010) The effects of salinity on nitrogen losses from an oligohaline estuarine sediment. Estuar Coasts 33:1054–1068. https://doi.org/10.1007/s12237-010-9280-7
Giblin AE, Tobias CR, Song B, Weston N, Banta GT, Rivera-Monroy V (2013) The importance of dissimilatory nitrate reduction to ammonium (DNRA) in the nitrogen cycle of coastal ecosystems. Oceanography 26:124–131. doi:https://doi.org/10.5670/oceanog.2013.54
Gilbert F, Souchu P, Bianchi M, Bonin P (1997) Influence of shellfish farming activities on nitrification, nitrate reduction to ammonium and denitrification at the water-sediment interface of the Thau lagoon, France. Mar Ecol Prog Ser 151:143–153. doi:https://doi.org/10.3354/meps151143
Goolsby DA, Battaglin WA, Aulenbach BT, Hooper RP (2000) Nitrogen flux and sources in the Mississippi River Basin. Sci Total Environ 248:75–86. doi:https://doi.org/10.1016/S0048-9697(99)00532-X
Hardison AK, Algar CK, Giblin AE, Rich JJ (2015) Influence of organic carbon and nitrate loading on partitioning between dissimilatory nitrate reduction to ammonium (DNRA) and N_2 production. Geochim Cosmochim Acta 164:146–160. doi:https://doi.org/10.1016/j.gca.2015.04.049
Henry KM (2012) Linking nitrogen biogeochemistry to different stages of wetland soil development in the Mississippi River delta, Louisiana. Dissertation, Louisiana State University
Henry KM, Twilley RR (2014) Nutrient biogeochemistry during the early stages of delta development in the Mississippi River deltaic plain. Ecosystems 17:327–343. https://doi.org/10.1007/s10021-013-9727-3
Hiatt M, Passalacqua P (2015) Hydrological connectivity in river deltas: the first-order importance of channel-island exchange. Water Resour Res 51:2264–2282. https://doi.org/10.1002/2014WR016149
Hiatt M, Castañeda-Moya E, Twilley R, Hodges BR, Passalacqua P (2018) Channel-island connectivity affects water exposure time distributions in a coastal river delta. Water Resour Res 54:2212–2232. https://doi.org/10.1002/2017WR021289
Hillebrand H, Sommer U (1999) The nutrient stoichiometry of benthic microalgal growth: Redfield proportions are optimal. Limnol Oceanogr 44:440–446. doi:https://doi.org/10.4319/lo.1999.44.2.0440
Howarth RW, Marino R, Cole JJ (1988) Nitrogen fixation in freshwater, estuarine, and marine ecosystems. 2. Biogeochemical controls. Limnol Oceanogr 33:688–701. doi:https://doi.org/10.4319/lo.1988.33.4_part_2.0688
Howarth RW, Sharpley A, Walker D (2002) Sources of nutrient pollution to coastal waters in the United States: implications for achieving coastal water quality goals. Estuaries 25:656–676. https://doi.org/10.1007/BF02804898
Jordan SJ, Stoffer J, Nestlerode JA (2011) Wetlands as sinks for reactive nitrogen at continental and global scales: a meta-analysis. Ecosystems 14:144–155. https://doi.org/10.1007/s10021-010-9400-z
Kana TM, Darkangelo C, Hunt MD, Oldham JB, Bennett GE, Cornwell JC (1994) Membrane inlet mass spectrometer for rapid high-precision determination of N_2, O_2, and Ar in environmental water samples. Anal Chem 66:4166–4170
Kana TM, Sullivan MB, Cornwell JC, Groszkowski KM (1998) Denitrification in estuarine sediments determined by membrane inlet mass spectrometry. Limnol Oceanogr 43:334–339. doi:https://doi.org/10.4319/lo.1998.43.2.0334
Koop-Jakobsen K, Giblin AE (2009) Anammox in tidal marsh sediments: the role of salinity, nitrogen loading, and marsh

vegetation. Estuar Coasts. https://doi.org/10.1007/s12237-008-9131-y

Koop-Jakobsen K, Giblin AE (2010) The effect of increased nitrate loading on nitrate reduction via denitrification and DNRA in salt marsh sediments. Limnol Oceanogr 55:789–802. doi:https://doi.org/10.4319/lo.2009.55.2.0789

Lane RR, Day JW, Marx B, Reyes E, Kemp GP (2002) Seasonal and spatial water quality changes in the outflow plume of the Atchafalaya River, Louisiana, USA. Estuaries 25:30–42. doi:https://doi.org/10.1007/BF02696047

Lorenzo-Trueba J, Voller VR, Paola C, Twilley RR, Bevington AE (2012) Exploring the role of organic matter accumulation on delta evolution. J Geophys Res Earth Surf 117:F4. https://doi.org/10.1029/2012JF002339

Ma H, Larsen LG, Wagner RW (2018) Ecogeomorphic feedbacks that grow deltas. J Geophys Res Earth Surf 123:3228–3250. https://doi.org/10.1029/2018JF004706

Michener WK, Blood ER, Bildstein KL, Brinson MM, Gardner LR (1997) Climate change, hurricanes and tropical storms, and rising sea level in coastal wetlands. Ecol Appl 7:770–801. doi:https://doi.org/10.1016/s1240-1307(97)87735-7

Miller-Way T, Twilley RR (1996) Theory and operation of continuous flow systems for the study of benthic-pelagic coupling. Mar Ecol Prog Ser 140:257–269. doi:https://doi.org/10.3354/meps140257

Mitsch WJ, Day JW, Zhang L, Lane RR (2005) Nitrate-nitrogen retention in wetlands in the Mississippi River Basin. Ecol Eng 24:267–278. doi:https://doi.org/10.1016/j.ecoleng.2005.02.005

Mulholland MR, Ohki K, Capone DG (2001) Nutrient controls on nitrogen uptake and metabolism by natural populations and cultures of Trichodesmium (Cyanobacteria). J Phycol 37:1001–1009. doi:https://doi.org/10.1046/j.1529-8817.2001.00080.x

Nielsen LP (1992) Denitrification in sediment determined from nitrogen isotope pairing. FEMS Microbiol Ecol 86:357–362. doi:https://doi.org/10.1111/j.1574-6968.1992.tb04828.x

Nielsen LP, Glud RN (1996) Denitrification in a coastal sediment measured in situ by the nitrogen isotope pairing technique applied to a benthic flux chamber. Mar Ecol Prog Ser 137:181–186. doi:https://doi.org/10.3354/meps137181

Noe GB, Hupp CR (2005) Carbon, nitrogen, and phosphorus accumulation in floodplains of Atlantic Coastal Plain rivers, USA. Ecol Appl 15:1178–1190. doi:https://doi.org/10.1890/04-1677

Noe GB, Hupp CR (2009) Retention of riverine sediment and nutrient loads by coastal plain floodplains. Ecosystems 12:728–746. https://doi.org/10.1007/s10021-009-9253-5

Noe GB, Hupp CR, Rybicki NB (2013) Hydrogeomorphology influences soil nitrogen and phosphorus mineralization in floodplain wetlands. Ecosystems 16:75–94. doi:https://doi.org/10.1007/s10021-012-9597-0

Ogilvie B, Nedwell DB, Harrison RM, Robinson A, Sage A (1997) High nitrate, muddy estuaries as nitrogen sinks: the nitrogen budget of the River Colne Estuary (United Kingdom). Mar Ecol Prog Ser 150:217–228. doi:https://doi.org/10.3354/meps150217

Paerl HW, Dennis RL, Whitall DR (2002) Atmospheric deposition of nitrogen: implications for nutrient over-enrichment of coastal waters. Estuaries 25:677–693. https://doi.org/10.1007/BF02804899

Patrick WH, Reddy KR (1976) Nitrification denitrification reactions in flooded soils and water bottoms: dependence on oxygen supply and ammonium diffusion. J Environ Qual 5:469–472. https://doi.org/10.2134/jeq1976.00472425000500040032x

Piña-Ochoa E, Álvarez-Cobelas M (2006) Denitrification in aquatic environments: a cross-system analysis. Biogeochemistry 81:111–130. https://doi.org/10.1007/s10533-006-9033-7

Pinay G, Clément JC, Naiman RJ (2002) Basic principles and ecological consequences of changing water regimes on nitrogen cycling in fluvial systems. Environ Manage 30:481–491. doi:https://doi.org/10.1007/s00267-002-2736-1

Ptacnik R, Andersen T, Tamminen T (2010) Performance of the Redfield ratio and a family of nutrient limitation indicators as thresholds for phytoplankton N vs. P limitation. Ecosystems 13:1201–1214. doi:https://doi.org/10.1007/s10021-010-9380-z

Rabalais NN, Turner RE, Dortch Q, Justic D, Bierman VJ, Wiseman WJ (2002) Nutrient-enhanced productivity in the northern Gulf of Mexico: past, present and future. Hydrobiologia 475–476:39–63. https://doi.org/10.1023/A:1020388503274

Redfield AC (1934) The haemocyanins. Biol Rev 9:175–212. https://doi.org/10.1111/j.1469-185X.1934.tb01002.x

Redfield AC (1958) The biological control of chemical factors in the environment. Am Sci 46:205–221. doi:https://doi.org/10.2307/27828530

Roberts HH, Walker N, Cunningham R, Kemp GP, Majersky S (1997) Evolution of sedimentary architecture and surface morphology: atchafalaya and Wax Lake Deltas, Louisiana (1973–1994). Gulf Coast Assoc Geol Soc Trans 47:477–484

Roberts HH, Coleman JM, Bentley SJ, Walker N (2003) An embryonic major delta lobe: a new generation of delta studies in the Atchafalaya-Wax lake delta system. Gulf Coast Assoc Geol Soc Trans 53:690–703

Ruehlmann J, Körschens M (2009) Calculating the effect of sediment organic matter concentration on soil bulk density. Soil Sci Soc Am J 73:876–885. doi:https://doi.org/10.2136/sssaj2007.0149

Scaroni AE, Nyman JA, Lindau CW (2011) Comparison of denitrification characteristics among three habitat types of a large river floodplain: Atchafalaya river basin. Louis Hydrobiol 658:17–25. https://doi.org/10.1007/s10750-010-0471-9

Scott JT, McCarthy MJ, Gardner WS, Doyle RD (2008) Denitrification, dissimilatory nitrate reduction to ammonium, and nitrogen fixation along a nitrate concentration gradient in a created freshwater wetland. Biogeochemistry 87:99–111. doi:https://doi.org/10.1007/s10533-007-9171-6

Seitzinger SP, Nixon SW, Pilson MEQ (1984) Denitrification and nitrous oxide production in a coastal marine ecosystem. Limnol Oceanogr 29:73–83. doi:https://doi.org/10.4319/lo.1984.29.1.0073

Shaw JB, Mohrig D, Whitman SK (2013) The morphology and evolution of channels on the Wax Lake Delta, Louisiana, USA. J Geophys Res Earth Surf. https://doi.org/10.1002/jgrf.20123

Sundback K, Enoksson V, Graneli W, Pettersson K (1991) Influence of sublittoral microphytobenthos on the oxygen and nutrient flux between sediment and water: a laboratory continuous- flow study. Mar Ecol Prog Ser 74:263–279. doi:https://doi.org/10.3354/meps074263

Syvitski JPM, Kettner AJ, Overeem I, Hutton EWH, Hannon MT, Brakenridge GR, Day H, Vörösmarty C, Saito Y, Giosan L, Nicholls R (2009) Sinking deltas due to human activities. Nat Geosci 2:681–686. doi:https://doi.org/10.1038/ngeo629

Trimmer M, Nicholls JC, Deflandre B (2003) Anaerobic ammonium oxidation measured in sediments along the Thames Estuary, United Kingdom. Appl Environ Microbiol 69:6447–6454. https://doi.org/10.1128/AEM.69.11.6447-6454.2003

Twilley RR, Bentley SJ, Chen Q, Edmonds DA, Hagen SC, Lam NSN, Willson CS, Xu K, Braud D, Peele RH, McCall A (2016) Co-evolution of wetland landscapes, flooding, and human settlement in the Mississippi River Delta Plain. Sustain Sci 11:711–731. doi:https://doi.org/10.1007/s11625-016-0374-4

Twilley RR, Day JW, Bevington AE, Castañeda-Moya E, Christensen A, Holm G, Heffner LR, Lane R, McCall A, Aarons A, Li S, Freeman A, Rovai AS (2019) Ecogeomorphology of coastal deltaic floodplains and estuaries in an active delta: Insights from the Atchafalaya Coastal Basin. Estuar Coast Shelf Sci. https://doi.org/10.1016/j.ecss.2019.106341

Vörösmarty CJ, Syvitski J, Day J, Sherbinn AD, Giosan L, Paola C (2009) Battling to save the world's river deltas. Bull Atom Sci 65:31–43

Wang S, Zhu G, Peng Y, Jetten MSM, Yin C (2012) Anammox bacterial abundance, activity, and contribution in riparian sediments of the Pearl River estuary. Environ Sci Technol 46:8834–8842. doi:https://doi.org/10.1021/es3017446

Wellner R, Beaubouef R, Van Wagoner J, Roberts H, Sun T (2005) Jet-plume depositional bodies-the primary building blocks of Wax Lake Delta. Gulf Coast Assoc Geol Soc Trans 55:867–909

Welti N, Bondar-Kunze E, Singer G, Tritthart M, Zechmeister-Boltenstern S, Hein T, Pinay G (2012) Large-scale controls on potential respiration and denitrification in riverine floodplains. Ecol Eng 42:73–84. doi:https://doi.org/10.1016/j.ecoleng.2012.02.005

White DA (1993) Vascular plant community development on mudflats in the Mississippi River delta, Louisiana USA. Aqua Bot 45:171–194. https://doi.org/10.1016/0304-3770(93)90020-W

White JR, DeLaune RD, Justic D, Day JW, Pahl J, Lane RR, Boynton WR, Twilley RR (2019) Consequences of Mississippi River diversions on nutrient dynamics of coastal wetland soils and estuarine sediments: a review. Estuar Coast Shelf Sci 224:209–216. https://doi.org/10.1016/j.ecss.2019.04.027

Xu YJ (2006) Total nitrogen inflow and outflow from a large river swamp basin to the Gulf of Mexico. Hydrol Sci J 51:531–542. doi:https://doi.org/10.1623/hysj.51.3.531

Yin G, Hou L, Liu M, Liu Z, Gardner WS (2014) A novel membrane inlet mass spectrometer method to measure $^{15}NH_4^+$ for isotope-enrichment experiments in aquatic ecosystems. Environ Sci Technol 48:9555–9562. doi:https://doi.org/10.1021/es501261s

Yu K, DeLaune RD, Boeckx P (2006) Direct measurement of denitrification activity in a Gulf coast freshwater marsh receiving diverted Mississippi River water. Chemosphere 65:2449–2455. https://doi.org/10.1016/j.chemosphere.2006.04.046